

Neutron scattering studies on stripe phases in non-cuprate materials

Holger Ulbrich^a, Markus Braden^a

^a*II. Physik. Institut, Universität zu Köln, Zùlpicher Str. 77, D-50937 Köln, Germany*

Abstract

Several non-cuprates layered transition-metal oxides exhibit clear evidence for stripe ordering of charges and magnetic moments. Therefore, stripe order should be considered as the typical consequence of doping a Mott insulator, but only in cuprates stripe order or fluctuating stripes coexist with metallic properties. A linear relationship between the charge concentration and the incommensurate structural and magnetic modulations can be considered as the finger print of stripe ordering with localized degrees of freedom. In nickelates and in cobaltates with K_2NiF_4 structure, doping suppresses the nearest-neighbor antiferromagnetism and induces stripe order. The higher amount of doping needed to induce stripe phases in these non-cuprates series can be attributed to reduced charge mobility. Also manganites exhibit clear evidence for stripe phases with further enhanced complexity, because orbital degrees of freedom are involved. Orbital ordering is the key element of stripe order in manganites since it is associated with the strongest structural distortion and with the perfectly fulfilled relation between doping and incommensurability. Magnetic excitations in insulating stripe phases exhibit strong similarity with those in the cuprates, but only for sufficiently short magnetic correlation lengths reflecting well-defined magnetic stripes that are only loosely coupled.

Keywords:

1. Introduction

The discovery of stripe-like magnetic and charge order in Nd-codoped $La_{2-x}Sr_xCuO_4$ [1] had a strong impact on the understanding about doping a Mott insulator. Several theoretical papers dealt with the introduction of charges into the Hubbard model and discussed the possibility of holes condensing into domain walls of the antiferromagnetic ordering [2–6]. Charged domain walls were found to be stable solutions of the still simple models even without taking an electron-phonon coupling into account [2–6]. The experimental confirmation of stripes in some cuprates materials inspired speculations about the role fluctuating charge inhomogeneity - or more specifically fluctuating stripes - could play in the superconducting pairing mechanism [7, 8] but this question still remains matter of controversy. In the cuprates, static stripe order competes with superconductivity, since the superconducting transition temperatures and the condensation energy are strongly suppressed in materials exhibiting static stripe order [9–12]. However, fluctuating stripe order can coexist with stable high-temperature superconductivity and be involved in the pairing [8]. In several cuprates, the dispersion of magnetic excitations shows a very characteristic hourglass shape [13–18] which can easily be explained by magnetic stripe ordering or by slowly fluctuating stripes. However, a successful description of the magnetic fluctuations is also obtained by the opposite scenario with itinerant charge carriers [19].

In order to better understand the role of the stripe instability in the physics of high-temperature superconductivity it seems

most interesting to investigate stripes phases in related compounds. By now, stripe-like charge and magnetic order were reported in several other transition-metal oxides with layered [20–22] or pseudo-cubic structure [23–25]. Fig. 1 illustrates the real-space ordering of the different stripe phases discussed for these materials together with the indication of the positions of superstructure reflections arising from magnetic and electronic ordering. These schemes which are frequently discussed in the literature, however, largely oversimplify the true ordering. Charge ordering like in most transition-metal oxides does not correspond to an integer modulation of the electron count at the metal site, and the charge modulation is not limited to the metal site [26] but most of the varying hole density sits on the bonds and ligands surrounding a metal site. Nevertheless these simple pictures give the clearest insight to the sometimes complex ordering schemes.

In the cuprates with large doping, charges are found to segregate in stripes running along the Cu-O bonds and are therefore called horizontal (or vertical) stripes [27]. In the nickelates stripes are observed to run along the diagonals (diagonal stripes) as it is also reported for low-doped $La_{2-x}Sr_xCuO_4$ [28–33]. The regular stacking of the stripes gives rise to superstructure-reflection intensities displaced by a propagation vector ϵ_{ch} from the Bragg peaks. Throughout the paper we give reciprocal space vectors in reduced lattice units referring to the small perovskite mesh with a lattice constant of ~ 3.8 Å. The commensurate arrangements in Fig. 1 explains that the in-plane length of ϵ_{ch} must be proportional to $1/n$ with n the stripe distance given in d-spacings of the corresponding planes. If the average stripe distance is incommensurate the resulting superstructure is incommensurate as well. In real space this just

Email address: braden@ph2.uni-koeln.de (Markus Braden)

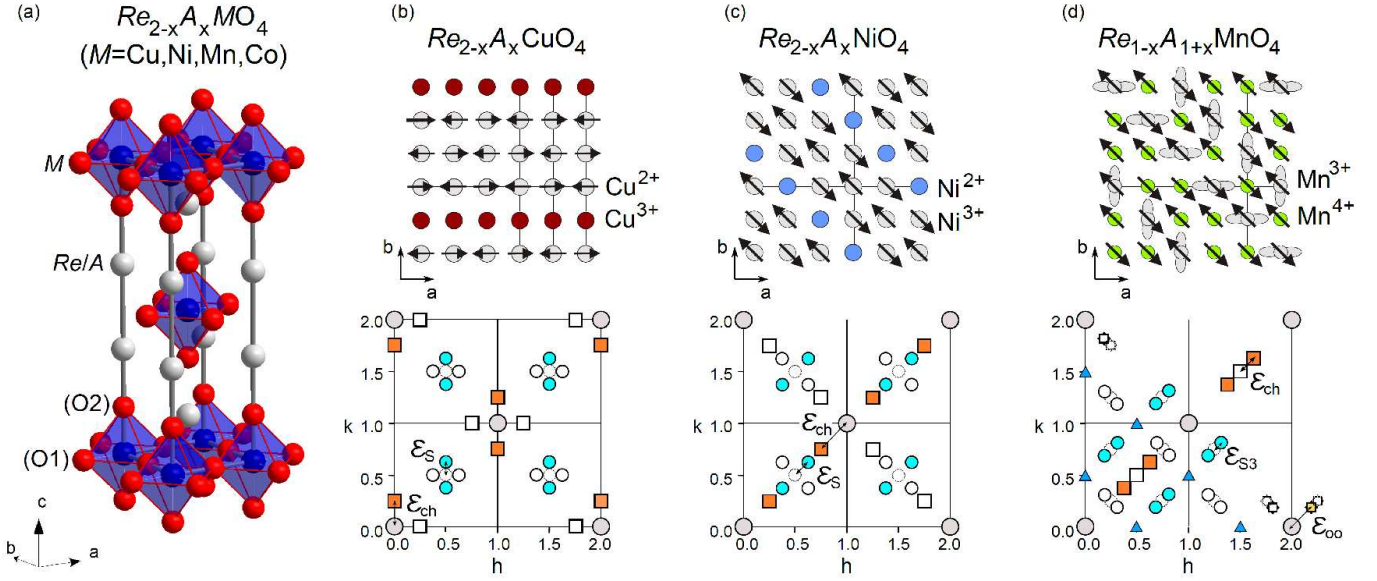


Figure 1: Crystal structure of $Re_{2-x}A_xMO_4$ with $Re = \text{La}$ or a rare earth, $A = \text{Sr}$ or Ca and $M = \text{Cu, Ni, Co, Mn}$. (Upper panels) Real-space drawings (ab-plane) of the schematic ordering of charges, magnetic moments and orbitals proposed for cuprates (b), nickelates (c) and manganites (d). In cuprates and nickelates regions of nn antiferromagnetism are separated by the charged stripes which act as domain walls. In layered manganites it is important to take the orbital degree of freedom at the nominal Mn^{3+} site into account, because this mediates the strongest ferromagnetic interaction. (Lower panels) The reciprocal space pictures for the purely two-dimensional ordering depicted above. For cuprates and nickelates charge and magnetic modulation yield corresponding scattering at satellites displaced from the original Bragg positions by ϵ_{ch} and ϵ_S , respectively. In the stripe ordering in layered manganites (c) charges, orbital and magnetic moments give rise to four different types of super-structure scattering associated with charge, orbital, Mn^{3+} - and Mn^{4+} -moment ordering.

means that the stripe distance varies on the local scale and that only the mean stripe distance is defined by the doping. This arrangement can be considered as a soliton lattice. Since the stripe distance in this simple model is just given by the amount of additional charges, it must amount to $n = 1/n_h$ times the d-spacing of the lattice with n_h the charge concentration. The length of ϵ_{ch} itself is then proportional to n_h . In stoichiometric $\text{La}_{2-x}\text{Sr}_x\text{NiO}_4$ we thus expect $\epsilon_{ch} = (x, x, q_l)$. In the horizontal or vertical stripes in the cuprates, one hole seems to occupy two sites and one gets $\epsilon_{ch} = (0.5 \cdot n_h, 0, q_l)$. In most cases, the fundamental structure is tetragonal and, therefore, unable to pin the stripe direction along a certain direction, or stripes in neighboring planes run in perpendicular direction. Therefore, the low-temperature scattering pattern consists of the superposition of at least two domain orientations with stripes running along perpendicular directions. Neutron diffraction is not directly sensitive to the electronic charges. However, a charge modulation on the metal site implies a modulation of the bond distances via the well-known relations between bond length and bond strength. This bond-length modulation can be analyzed through the displacements of the oxygen atoms. Since neutron scattering is more sensitive on the oxygen than x-rays, the precise determination of the charge-order related distortion can be more easily performed with neutron diffraction techniques [34]. Direct insight can, however, be obtained when using resonant x-ray diffraction in particular in the soft energy range [35]. Neutron diffraction thus senses the lattice distortions generated by the charge ordering. Since this is not a scalar scattering contribution the charge-order related intensities can only be observed

at positions with finite structure factor. For the charge ordering we essentially expect a breathing-type distortion which in general can be studied only in an at least partially longitudinal configuration [36, 37].

As the stripe acts as a domain wall for the antiferromagnetic order between two charge stripes, the wave length of the magnetic modulation is twice as large as the structural one. Magnetic super-structure intensities appear thus at positions shifted by ϵ_S from the magnetic Bragg peak of the commensurate nearest-neighbor antiferromagnetic order at $(0.5, 0.5, q_l)$, and the in-plane length of ϵ_S is just half that of ϵ_{ch} : $\epsilon_S = \frac{1}{2} \cdot \epsilon_{co}$. This resembles the situation in a classical spin-density wave (SDW) like that in Cr where a coupling with a structural modulation with half period arises from the magnetostriction [38–40]. The crystal structure distorts in the way, that the magnetic interaction is enhanced in regions of large moments and reduced in regions of low moments. The doubling of the nuclear modulation vector with respect to the magnetic one, arises from the fact that the magnetostriction does not depend on the sign of the moments and that the real-space wave length is therefore half as long. The coupled charge and magnetic order in the cuprates and in the nickelates as well as the charge orbital and magnetic ordering in the manganites can in principle be interpreted in such SDW and charge-density wave (CDW) model, but the larger amount of experiments point to the local stripe model at least for the insulating materials discussed here. In particular the clear relation between the incommensurability and the charge concentrations, which is well fulfilled in nickelates, cobaltates and manganites, is difficult to explain with a

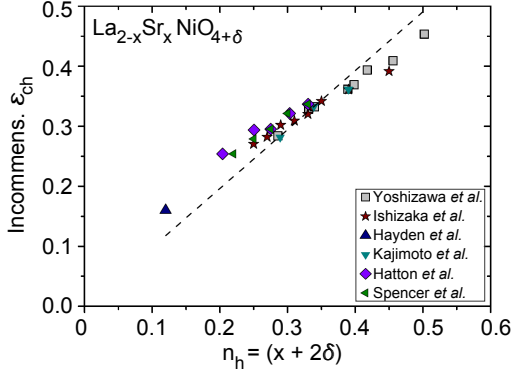


Figure 2: Dependence of the incommensurate modulation of spin and nuclear structure on the hole concentration $n_h = x + 2 \cdot \delta$ in $\text{La}_{2-x}\text{Sr}_x\text{NiO}_{4+\delta}$, data are taken from [56, 69, 72, 73, 76, 77] and correspond to the low-temperature values. Note that the incommensurability is not exactly following $\varepsilon_{ch} = n_h$ (indicated by the dashed line), but the incommensurability tends to approach $\varepsilon_{ch} \sim \frac{1}{3}$.

SDW-CDW model basing on a Fermi-surface instability.

The diagonal stripe pattern shown in Fig. 1(c) applies to the nickelates and most likely also to the layered cobaltates [21] and low-doped cuprates [28–33]. Stripe ordering in manganites was first reported for the pseudo-cubic perovskite phases [23–25]. These materials are, however, heavily twinned rendering the interpretation of any neutron scattering experiments very difficult. Therefore, a fully consistent picture could only be established for a layered manganite, $\text{La}_{0.42}\text{Sr}_{1.58}\text{MnO}_4$, which was slightly overdoped in respect to the stable ordering at half doping [22]. The orbital degree of freedom plays an important role in the ordering processes in the manganites, whereas it is fully suppressed in the cuprates. This considerably enhances the complexity of the stripe order in the manganites, see Fig. 1(d). Another difference concerns the doping range where stripe patterns are observed. In the cuprates stripes appear at rather low doping and thus close to the simple nn antiferromagnetic phase. In nickelates and cobaltates the stripe magnetic ordering is seen already at higher doping but it is still possible to associate the stripe modulation with the nn antiferromagnetism in the parent compounds. In the layered manganites one typically considers LaSrMnO_4 with only Mn^{3+} (with a $3d^4$ electronic configuration) as the starting material. Doping leads to the suppression of the nn AFM order in LaSrMnO_4 and to a quite stable charge, orbital, and magnetic order at half doping, $\text{La}_{0.5}\text{Sr}_{1.5}\text{MnO}_4$, where orbital order seems to be essential for the magnetic interaction. In this phase ferromagnetic zigzag chains are coupled antiferromagnetically; this magnetic arrangement is called CE-type. Stripe-like ordering of the various degrees of freedom develops in the manganites only in relation with the CE-type order at half doping, see Fig. 1(d).

In this article we will resume the overwhelming amount of work performed on the stripe phases in nickelates and compare the results with the properties of the more recently reported stripe ordering in layered cobaltates and manganites.

2. Stripe order of charges and magnetic moments in layered nickelates

After the discovery of superconductivity in the cuprates, the electronic properties of layered nickelates were studied as well, but metallic behavior can be induced only for very high amounts of doping, $x \sim 1$, in $\text{La}_{2-x}\text{Sr}_x\text{NiO}_4$ [41, 42]. The low conductivity in $\text{La}_{2-x}\text{Sr}_x\text{NiO}_4$ at moderate doping is attributed to the formation of small polarons [43, 44]. Besides the interest in the stripe ordering of charges and electrons discussed here, doped nickelates attract strong attention due to the observation of an electric-field driven brake down of the insulating state [45], due to a dielectric anomaly reflecting the glassy electronic state [46], and most recently due to the hole Fermi surface observed for a $d_{x^2-y^2}$ band in highly doped materials [47].

Pure La_2NiO_4 can be doped either by Sr or Ca substitution or by insertion of excess oxygen leading to $\text{La}_{2-x}\text{Sr}_x\text{NiO}_{4+\delta}$ [41, 42, 48]. The precise control of the oxygen stoichiometry is particularly difficult during the growth of single crystals strongly affecting the reliability of the absolute value of the total charge concentration, $n_h = x + 2\delta$ in $\text{La}_{2-x}\text{Sr}_x\text{NiO}_{4+\delta}$. Synthesizing stoichiometric $\text{La}_{2-x}\text{Sr}_x\text{NiO}_4$ becomes more difficult with decreasing Sr content, since these compounds easily incorporate large amounts of excess oxygen [49].

Pure La_2NiO_4 exhibits a structural phase transition from the high-temperature tetragonal (HTT) phase to a low-temperature orthorhombic (LTO) phase [50] like pure La_2CuO_4 , but due to higher bond-length mismatch the transition occurs at higher temperature in La_2NiO_4 , $T_{LTO} \sim 781$ K [51]. At 70 K a second structural phase transition occurs into a low-temperature tetragonal (LTT) phase [52]. The LTO and LTT phases are both characterized by tilting of the NiO_6 octahedra but the tilt axes differ: In the LTO phase the tilt axis is along the diagonals of the small perovskite (or parallel to NiO_6 octahedron edge), whereas octahedra tilt around an axis parallel to the bond in the LTT phase. Monoclinic phases with the tilt axis oriented near but not exactly along the bonds are labelled low-temperature less orthorhombic (LTLO). The structural distortion is suppressed by the Sr doping [51, 53] as it is expected by the bond-length mismatch model due to the large ionic radius of Sr and due to the oxidation of Ni similar to the case of $\text{La}_{2-x}\text{Sr}_x\text{CuO}_4$ [54, 55]. La_2NiO_4 exhibits nn antiferromagnetic order below $T_N \sim 650$ K with an ordered moment of $1.6 \mu_B$ [52] in reasonable agreement with the expectation for $S = 1$ Ni^{2+} with $3d^8$ configuration.

First evidence for an incommensurate magnetic correlation was obtained in an elastic neutron-scattering study on $\text{La}_{1.8}\text{Sr}_{0.2}\text{NiO}_4$ and antiphase domain walls were discussed as one possible explanation [56]. This crystal was annealed at highly reducing conditions resulting in an oxygen content of 3.96(6). Furthermore, electron diffraction experiments on several $\text{La}_{2-x}\text{Sr}_x\text{NiO}_4$ crystals revealed quasi-2D superlattice peaks whose positions strongly depend on the Sr concentration [57]. A study of the x-ray scattering on comparable crystals revealed strong diffuse contributions at symmetric satellite positions which, however, cannot be explained with the charge correlations and may result from thermal diffuse scattering or

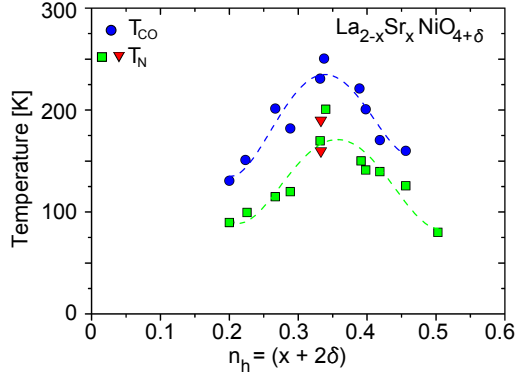


Figure 3: Transition temperatures into the charge (T_{CO}) and magnetic (T_N) ordered states plotted against the hole concentration $n_h = x + 2 \cdot \delta$, data from [69]. The red triangles indicate neutron and NMR measurement of T_N of the same sample indicating that magnetic order is not fully static below the T_N observed in neutron scattering experiments but fluctuating with a slow time scale [67, 80].

some La Sr ordering [58]. For an oxygen-doped crystal of $\text{La}_2\text{NiO}_{4.125}$, Yamada et al. find incommensurate magnetic scattering to appear at rather high temperature in view of the large amount of doping [59]. For the same material Tranquada et al. established for the first time the simultaneous ordering of holes and spins according to the pattern shown in Fig. 1(c) which precisely corresponds to the hole concentration of $n_h = 0.25$ in this material [60]. The excess oxygen in $\text{La}_2\text{NiO}_{4+\delta}$ orders upon cooling giving rise to very complex phase diagrams and to a variety of superstructure reflections which superpose or overlap with those associated with the charge and spin stripe ordering [61–63]. Magnetic moments in $\text{La}_2\text{NiO}_{4.125}$ align perpendicular to the modulation, i.e. parallel to the stripes, and are pretty large, about 80% of the ordered moment in pure La_2NiO_4 [63]. A more stable charge order was detected for higher amount of excess oxygen similar to the later observation on $\text{La}_{2-x}\text{Sr}_x\text{NiO}_4$ [64, 65] and allowed for a better characterization of the underlying structural distortion. The charge incommensurability is not constant in this material but discontinuously varies upon cooling passing through several commensurate lock-in values as in a typical incommensurate structural modulation [64].

The ordering of the excess oxygen, however, complicates the analysis of the magnetic order and of the corresponding excitations. Therefore, the larger part of neutron and x-ray scattering studies was performed on $\text{La}_{2-x}\text{Sr}_x\text{NiO}_{4+\delta}$ single crystals [20, 66–79]. In an oxygen-stoichiometric sample with $x = 0.2$ Tranquada et al. find the magnetic correlation at $\epsilon_S \sim (0.125, 0.125, l)$ peaking at odd l [66], but the modulation perpendicular to the planes remains quite weak. Charge scattering appears at $\epsilon_{ch} \sim (0.25, 0.25, l)$ again with odd l but is better defined along the c direction. Note that the incommensurability is slightly higher than expected for the amount of charges. For a crystal with the same Sr content but less oxygen Hayden et al. found an incommensurability of only $\epsilon_S \sim 0.08$ suggesting $\epsilon_{ch} \sim 0.16$ [56] slightly below the expected value. These two measurements illustrate the uncertainty arising from the oxygen concentration in these materials, but they both prove that the stripe

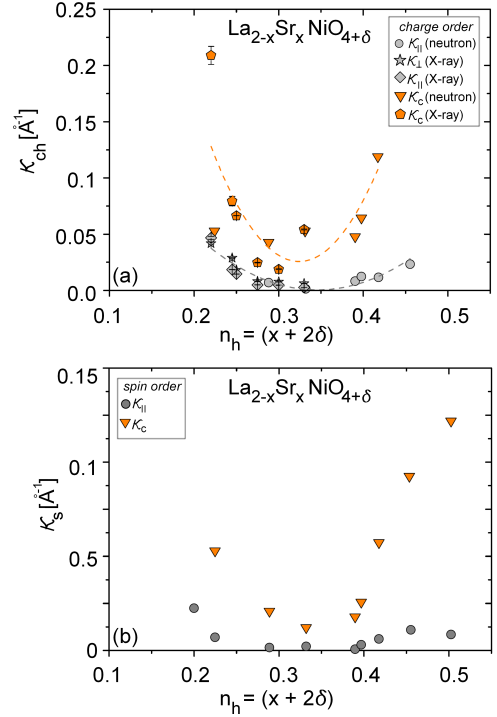


Figure 4: The inverse charge-correlation lengths along the stripe modulation in-plane, κ_{\parallel}^{ch} , perpendicular to the modulation but parallel to the planes κ_{\perp}^{ch} (note that this direction is parallel to the stripes), and perpendicular to the planes, κ_c^{ch} (above). The inverse magnetic correlation lengths are given below: parallel to the modulation, κ_{\parallel}^S , and perpendicular to the planes, κ_{\perp}^S . Data are taken from references [69, 77].

order of charges and spins in $\text{La}_{2-x}\text{Sr}_x\text{NiO}_{4+\delta}$ sets in for samples which still exhibit the structural distortion due to the octahedron tilting, $T_{HTT/LTO} \sim 70$ K in $\text{La}_{1.8}\text{Sr}_{0.2}\text{NiO}_4$ [66]. When scanned with energy analysis, elastic magnetic correlations appear below $T \sim 90$ K in $\text{La}_{1.8}\text{Sr}_{0.2}\text{NiO}_4$ [66] which is significantly below the charge ordering temperature, $T_{co} \sim 115$ K, in this material. This indicates that magnetic correlations become quasi-static on the time-scale of this experiment below $T \sim 90$ K (i.e. relaxation times are larger than a few ps). When scanning in an energy-integrating neutron-scattering mode, which is possible due to the 2D character of the signal, the magnetic signal in $\text{La}_{1.8}\text{Sr}_{0.2}\text{NiO}_4$ persists to higher temperature and seems to disappear together with the charge ordering. Charge order thus immediately triggers strong 2D magnetic correlations in $\text{La}_{2-x}\text{Sr}_x\text{NiO}_4$ but these remain inelastic till much lower temperature. The importance of time scales is further illustrated in a NMR study on $\text{La}_{1.67}\text{Sr}_{0.33}\text{NiO}_4$ which finds a 30K lower magnetic transition temperature than the neutron experiments due to the μs time scale of the NMR experiment [80]. Clearly, the magnetic transitions in $\text{La}_{2-x}\text{Sr}_x\text{NiO}_{4+\delta}$ possess a glassy character.

The Sr concentration of $x = 0.2$ is the lowest one, where stripe ordering has been unambiguously established [56] yielding the smallest modulation reported so far ($\epsilon_S \sim 0.08$). For the Sr content of $x = 0.135$ Tranquada et al. find static or quasistatic response at the commensurate position of the nn antiferromagnetism [66] suggesting that $\text{La}_{2-x}\text{Sr}_x\text{NiO}_4$ with $x = 0.135$ ex-

hibits glassy commensurate antiferromagnetism at a rather low T_N of 65 K. Also a study of the magnetic excitations for $x = 0.12$ showed the renormalized magnon dispersion expected for a commensurate structure [81, 82].

Systematic studies on the doping dependence of the stripe order in $\text{La}_{2-x}\text{Sr}_x\text{NiO}_{4+\delta}$ were performed by comprehensive neutron [69, 71, 73] and x-ray [72, 76–79] scattering studies. The resulting doping dependencies of the transition temperatures, of the incommensurabilities and of the inverse correlation lengths are shown in Figures 2,3 and 4, respectively. These studies document an enhanced stability of the stripe phase at $x = 1/3$. For this concentration the magnetic and charge ordering transition are the highest and the correlation lengths are the longest. Just the checkerboard charge ordering for half doping appears at even higher temperature but this phase is again commensurate. Evidence for the particular stability of the stripe phase at $x = 1/3$ is also found in the clear specific heat anomaly [44]. The magnetic structure of the $x = 1/3$ stripe phase is commensurate and quite simple as the magnetic cell comprises only two antiparallel magnetic moments, see Fig. 5 (a).

The incommensurability for $x = 1/3$ fits exactly the Sr content and does not vary with temperature. In addition, the in-plane correlation lengths are pretty large. For example the magnetic correlation length along the modulation vector amounts to $\xi_{\parallel}^S = 100 \text{ \AA}$ and that of the longitudinal charge modulation to $\xi_{\parallel}^{ch} = 350 \text{ \AA}$ while the modulations perpendicular to the planes are still limited and approximately equal $\xi_c^S \sim \xi_c^{ch} \sim 30 \text{ \AA}$ [67]. With synchrotron radiation the in-plane anisotropy of the charge superstructure was analyzed finding shorter correlation lengths along the stripe modulation vector than perpendicular to it, $\xi_{\parallel}^{ch} < \xi_{\perp}^{ch}$ for Sr concentrations between $x = 0.225$ and $x = 0.33$ [74–76], see Fig. 4. This anisotropy seems to be the direct consequence of the solitonic arrangement of the stripes. Locally, the distance between two Ni-centered charge stripes can only amount to an integer multiple but this number has to vary in order to adapt for the non-commensurate charge concentration generating some diffuse scattering. In contrast, along the stripes and thus perpendicular to the stripe modulation the order can be perfect in principle [83].

We note that charge-order superstructure scattering in $\text{La}_{2-x}\text{Sr}_x\text{NiO}_4$ always peaks at $(\varepsilon, \varepsilon, l)$ with odd l , whereas the magnetic scattering exhibits peaks for odd and even l [67, 71]. Due to the body centering of the small tetragonal cell of the K_2NiF_4 structure in $I4/mmm$, $(0, 0, 1)$ is not a Bragg point and the propagation vectors $(\varepsilon, \varepsilon, l)$ with odd and even l are not equivalent but refer to 180° or zero phase shift for the modulation of the two Ni sites at $(0, 0, 0)$ and at $(0.5, 0.5, 0.5)$, respectively. The Coulomb forces require always anti-phase stacking of the charge ordering in agreement with the finite dispersion of phonons perpendicular to the planes [84, 85]. In contrast, both in-phase and anti-phase magnetic stacking is possible. For $x = 0.333$ only a small amount of the even- l scattering is observed [67], but the relative weight of the even- l signals increases upon increase or reduction of the Sr content away from $x = 1/3$ [71] underlining the particular stability of the charge and magnetic order at this composition.

The relevance of the commensurate and stable $x = 1/3$ structure becomes further illustrated when looking at the temperature dependence of incommensurabilities [72, 73, 76]. The charge incommensurability is not constant but varies upon cooling as already observed earlier, and the comprehensive analyzes show that the temperature dependence is determined through the doping. For $x < 0.33$, ε_{ch} is much closer to $1/3$ at high temperatures than the doping suggests but ε_{ch} decreases on cooling approaching the expected value at low temperature; these low-temperature values are given in Fig. 2. For larger doping, $x > 1/3$, the same behavior is observed but it results in an increase of ε_{ch} upon cooling [72, 73]. This behavior points to an electronic self doping of the charge stripes at higher temperature [72, 73]. One may thus consider the variation of charge content around $x \sim n_h = 1/3$ as doping into the stable antiferromagnetic $x = \frac{1}{3}$ Mott state shown in Fig. 2. This picture is further corroborated by the Hall effect measurements across this amount of doping which show a change in the sign of charge carriers just at $x = 1/3$ and suggest electron- and hole-like charge carriers below and above this value, respectively [86]. The stability of the commensurate phase at $x = 1/3$ thus explains the slight deviations of the $\varepsilon_{ch} = n_h$ rule that persist even at low temperatures, see Fig. 2, but the overall correspondence between charge concentration and incommensurability yields a strong argument in favor of the stripe picture with localized charges and moments.

There is a discrepancy between the synchrotron and the neutron studies concerning the low-temperature behavior of the charge ordering. Upon cooling synchrotron experiments find a reduction of the peak height [76, 77, 79], which is accompanied by a broadening and a slight shift of the signal. The variation in the integrated intensity, therefore, is less dramatic. This behavior may arise from the freezing of the correlations into the intrinsic disorder of the materials combined with the different time- and spatial scales of neutron and synchrotron diffraction experiments but requires further attention.

Astonishingly little is known about the microscopic structure of the charge order in $\text{La}_{2-x}\text{Sr}_x\text{NiO}_4$. The average crystal structure in $\text{La}_{1.67}\text{Sr}_{0.33}\text{NiO}_4$ seems not to change when entering the charge-ordered phase [87, 88] but the distortions arising from the charge modulation have not been reported so far. This limits the reliability of density-functional theory (DFT) analyzes which need to determine the microscopic distortions by structure relaxation [89–91]. For an oxygen doped material, NMR experiments document the solitonic character and indicate that charge ordering is centered at the Ni sites with $S = \frac{1}{2}$ $\text{Ni}^{3+} 3d^7$ ions in the domain walls [92, 93]. Resonant diffraction experiments using soft x-ray for $\text{La}_{1.8}\text{Sr}_{0.2}\text{NiO}_4$ reveal that the holes are mainly located on oxygens surrounding a nominal Ni^{3+} and that the difference in electron counting is quite small, $\Delta Z \sim 0.3$ electron charges [78]. The magnetic structure in the stripe phase was studied by polarized and unpolarized-neutron diffraction revealing a spin reorientation transition within the ab plane for $x = 0.275, 0.37$, and 0.4 [94].

Various inelastic neutron scattering experiments were performed to study the magnon dispersion in pure La_2NiO_4 and in several stripe phases [81, 95–100]. Pure La_2NiO_4 exhibits

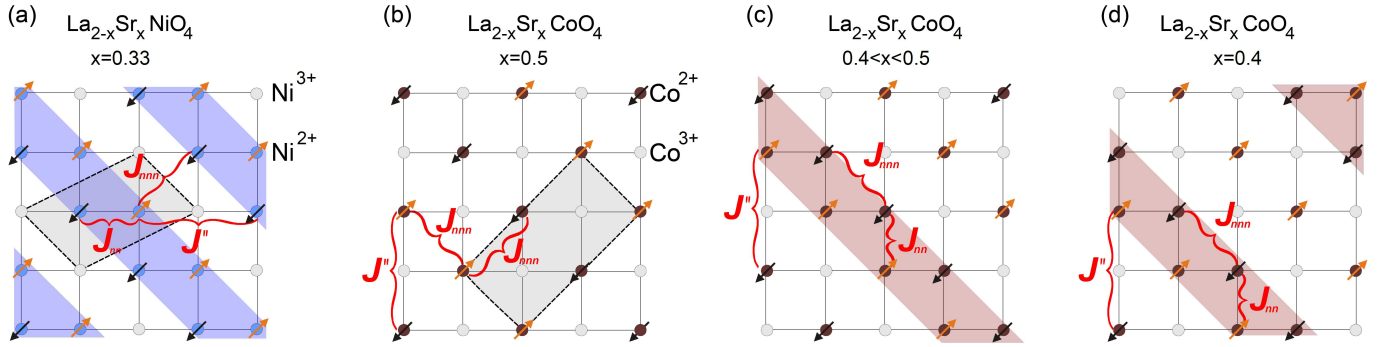


Figure 5: Scheme of the robust magnetic order occurring at $x = 1/3$ doping in the nickelates (a); magnetic interaction parameters are indicated, J_{nm} between neighboring Ni^{2+} ; J_{nm} and J'' describe the interaction across the charge stripe. (b)-(d) Scheme of the magnetic and charge ordering appearing in $\text{La}_{2-x}\text{Sr}_x\text{CoO}_4$. (b) ideal ordering at halfdoping $\text{La}_{1.5}\text{Sr}_{0.5}\text{CoO}_4$; charges order into a checkerboard arrangement with magnetic Co^{2+} and non-magnetic Co^{3+} sites; magnetic interaction parameters between magnetic Co^{2+} are indicated in the same notation as in part (a); (c) stripe-like modulation of the ordering slightly below half doping, where additional magnetic stripes stabilize magnetic ordering and (d) stripe order order for $x=0.4$.

a steep magnon dispersion with a spin-wave velocity of 340 meVÅ [95]. In a stripe phase with an oxygen excess of $\delta = 0.133$, spin-wave-like excitations still exhibit a steep dispersion emanating at the incommensurate magnetic zone centers with a spin-wave velocity reduced by 40 % compared to that in pure La_2NiO_4 [96]. Batista et al. proposed first that the magnon dispersion of a stripe phase can explain the peculiar resonance mode observed in the cuprates superconductors [101]. In a stripe phase, magnon branches emanate at four incommensurate spots surrounding the $(0.5, 0.5, 0)$ position of the nn commensurate antiferromagnetism; the merging of these contributions should result in a resonance-like intensity enhancement [101]. The magnon dispersion of the stripe phases in $\text{La}_{2-x}\text{Sr}_x\text{NiO}_4$ was therefore studied in great detail focusing on the concentration range near $x = 1/3$ [97–100]. For $x = 0.31$ close to the most stable order a steep dispersion was observed with an almost isotropic spin-wave velocity of about 320 meVÅ which is comparable to that in pure La_2NiO_4 [97]. This indicates that the magnetic coupling across the stripe (J_{nm} and J'' in Fig. 5) is quite strong in this simple magnetic structure. Further experiments show that essentially the same high-energy dispersion is observed when the doping is slightly varied [97–100]. These findings agree with the already mentioned dominance of the $x = 1/3$ phase in $\text{La}_{2-x}\text{Sr}_x\text{NiO}_4$ which seems to prohibit the emergence of a cuprate-like dispersion of magnetic excitations. Just half-doped $\text{La}_{1.5}\text{Sr}_{0.5}\text{NiO}_4$ with checkerboard arrangement exhibits a different dispersion of magnetic excitations [102, 103]. The $S = \frac{1}{2}$ Ni^{3+} ions in the domain walls can be considered as forming a chain-like magnetic arrangement and the characteristic features of such a chain indeed were found in the inelastic neutron scattering response [99, 104].

Stable stripe order was also found in $\text{Re}_{1.67}\text{A}_{0.33}\text{NiO}_4$ with Re a rare-earth element and $\text{A} = \text{Ca}$ or Sr [105–107]. The smaller ionic radius of the rare earth stabilizes the structural tilt distortion which pins the direction of the stripes along the direction of the octahedral tilt axis. The disorder induced by the local variation of the ionic radii at the Re site in $\text{Re}_{1.67}\text{A}_{0.33}\text{NiO}_4$ reduces the correlation lengths yielding the longest correlations

for $\text{Pr}_{1.67}\text{Ca}_{0.33}\text{NiO}_4$ [107]. These findings on materials with smaller ions occupying the Re site corroborate the conclusion in $\text{La}_{2-x}\text{Sr}_x\text{NiO}_4$ that stripe order can coexist with the tilt distortions.

Phonons in $\text{La}_{2-x}\text{Sr}_x\text{NiO}_{4+\delta}$ have been studied [84, 85] as reference to the cuprates high-temperature superconductors which exhibit strong phonon anomalies [108–119]. The lattice dynamics in the undoped parent compounds can be very well understood by ionic lattice-dynamics model [120], but in electronically doped cuprates, significant discrepancies appear in the dispersion of the longitudinal bond-stretching branches [108–119]. Including electronic screening to the models describing the lattice dynamics of the cuprates parent compounds yields an increasing dispersion for the longitudinal bond-stretching branches, since the screening is less perfect at small distances corresponding to larger phonon propagation vectors. Doped cuprates indeed show this behavior for several polar branches, but the longitudinal bond-stretching branches behave differently. They exhibit a nearly flat dispersion along [110] and even a decreasing dispersion along [100]. In the [100] direction a strongly renormalized half-breathing mode is observed together with strong frequency broadening. This anomaly can be identified with the tendency towards stripe ordering [36, 112, 119]. The phonon dispersion in doped nickelates is also anomalous, because longitudinal bond-stretching branches soften in the Brillouin zone [84, 85] so that the longitudinal breathing modes fall below the transverse bond-stretching modes, which can be considered as an overscreening effect. However, in contrast to the cuprates, the down-bending is not limited to the [100] direction but appears also for [110] where it is even stronger. This corroborates the general interpretation that the bond-stretching modes in transition-metal oxides dynamically reflect the charge ordering instabilities [36], because the charge-stripe modulation in nickelates appears along the [110] direction as well. The question whether there is a more direct signature of the charge stripe ordering in the phonon dispersion in $\text{La}_{2-x}\text{Sr}_x\text{NiO}_{4+\delta}$ requires further attention [81].

The schematic phase diagram of $\text{La}_{2-x}\text{Sr}_x\text{NiO}_4$ is shown in

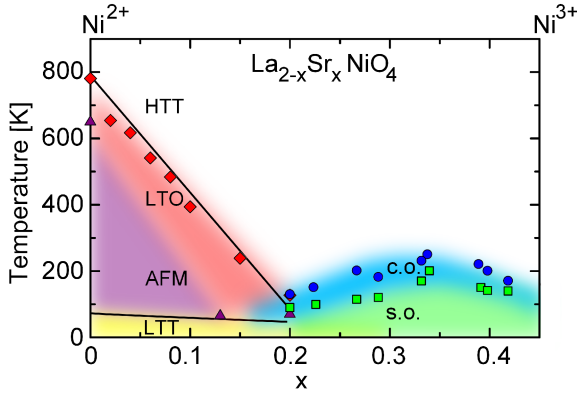


Figure 6: Phase diagram of $\text{La}_{2-x}\text{Sr}_x\text{NiO}_4$ concerning the structural distortion (red triangles and line), the suppression of commensurate antiferromagnetism (magenta triangles) and the appearance of the stripe phase with charge (blue) and magnetic (green) transitions. The LTT or LTLO phase is indicated in yellow. Data are taken from [51, 66, 69].

Fig. 6; the doping suppresses both the structural distortion and the commensurate nn antiferromagnetic order giving rise to the charge and spin stripe ordering. The crossover from the commensurate nn antiferromagnetism to the stripe order occurs near $x \sim 0.2$ close to the full suppression of the structural distortion, but there is overlap of the octahedron tilt distortion and the stripe phases [66].

3. Incommensurate magnetic order in layered cobaltates

In view of the enormous amount of literature on $\text{La}_{2-x}\text{Sr}_x\text{NiO}_4$ it is astonishing that the isostructural cobaltates, $\text{La}_{2-x}\text{Sr}_x\text{CoO}_4$, were only little studied. Similar to $\text{La}_{2-x}\text{Sr}_x\text{NiO}_4$, layered cobaltates do not become metallic unless a high amount of doping above $x \sim 1$ is introduced [121–124]. In the cobaltates one has to distinguish different possibilities to distribute the electrons in the t_{2g} and e_g crystal-field levels in an octahedral arrangement. Co^{2+} with seven electrons in the d shell always exhibits a high-spin (HS) $S = \frac{3}{2}$ state in an octahedral arrangement due to Hund's rule coupling [125]. In contrast, Co^{3+} with six electrons in the d shell can adopt different spin states depending on the number of electrons transferred to the higher e_g level: a low-spin (LS) non-magnetic state with all electrons in the t_{2g} level, an intermediate-spin (IS) state with $S = 1$ for one electron transferred to the e_g orbital, and a HS state with $S = 2$ for two transferred electrons. It is well known that the spin state of Co^{3+} may even vary as a function of temperature [126]. The possible spin-state transitions as a function of doping render the analysis of the phase diagram of $\text{La}_{2-x}\text{Sr}_x\text{CoO}_4$ more difficult and different spin-state scenarios were proposed [121, 127]. Similar to the nickelates, the layered cobaltates also tend to incorporate large amounts of excess oxygen rendering the growth of single crystals particularly difficult in the low-doping range [128–131] whereas powder samples can be more easily controlled [121, 132].

Pure La_2CoO_4 exhibits the HTT to LTO transition at a high temperature of 900 K [133] due to further increased bond-length mismatch. Upon cooling the second structural transition

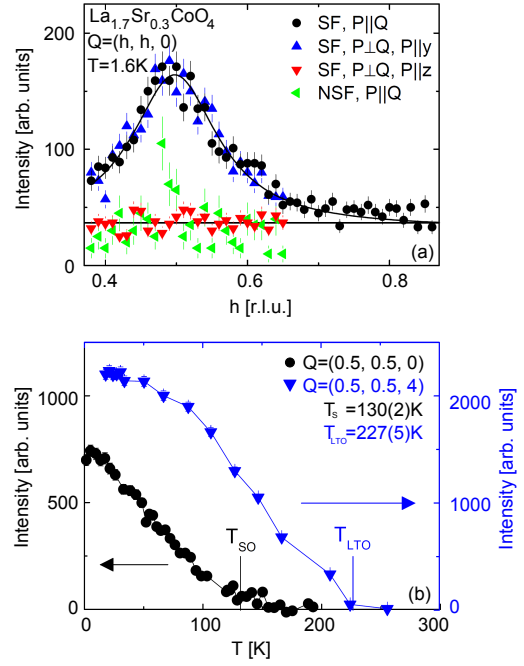


Figure 7: Magnetic ordering occurring in $\text{La}_{1.7}\text{Sr}_{0.3}\text{CoO}_4$ [21]; scans with neutron-polarization analysis are shown in part (a) documenting the magnetic nature of the very broad commensurate signal at low temperatures; the temperature dependencies of the structural and magnetic superstructure intensities are given in part (b).

to the LTT phase is found at 135 K, and nn antiferromagnetic order develops below 275 K [125]. The larger structural distortion in the cobaltates is reflected in a larger amount of Sr-doping needed to fully suppress the tilting of the octahedra: about 40% in the cobaltates versus slightly above 20% in the nickelates and cuprates. The single-layer magnetic structure of pure La_2CoO_4 , La_2NiO_4 , and La_2CuO_4 are identical but the direction of the ordered moment in the orthorhombic structure and the stacking of the magnetic layers is different. Adopting space group Bmab for the LTO phase, the spins point along the a direction for La_2CoO_4 and La_2NiO_4 ; note that the a direction is the tilt axis in Bmab. In La_2CuO_4 spins align along b perpendicular to the tilt axis, so that Dzyaloshinski-Moriya interaction gives rise to a small canting of magnetic moments along c [134]. The stacking of magnetic order in all three compounds is described by the $(1, 0, 0)$ vector which yields different magnetic structures due to the rotation of moments between La_2CuO_4 and $\text{La}_2\text{NiO}_4/\text{La}_2\text{CoO}_4$. The two types of structure are characteristic for many compounds with K_2NiF_4 structure and may even coexist [135].

At half-doping, $\text{La}_{1.5}\text{Sr}_{0.5}\text{CoO}_4$ exhibits checkerboard charge ordering at the exceptionally high transition temperature of $T_{CO} = 825(27)$ K. In this very stable charge ordered phase magnetic order develops only below $T_S \sim 30$ K [136, 137]. The large ratio of $T_{CO}/T_S \sim 30$ indicates an effective decoupling of the two phenomena and thus implies that in this cobaltate the charge order arises from electron-lattice coupling [137].

The spin state of Co^{3+} in the $\text{La}_{2-x}\text{Sr}_x\text{CoO}_4$ series has generated a lot of controversy following the initial analysis of Moritz

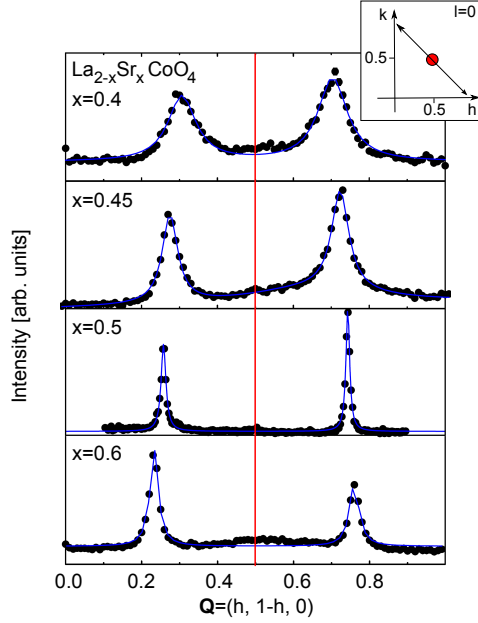


Figure 8: Elastic neutron scattering scans aiming at the magnetic ordering occurring in $\text{La}_{2-x}\text{Sr}_x\text{CoO}_4$; the scans connect two satellites depicted in Fig. 1(c) with the position of nn commensurate antiferromagnetism. Data taken from reference [21].

omo et al. proposing a HS to IS transition near $x = 0.7$ [121]. The magnetic structure analysis in $\text{La}_{1.5}\text{Sr}_{0.5}\text{CoO}_4$ indicates an effectively non-magnetic Co^{3+} and a rough study of the structural distortions was interpreted as evidence for an IS state. The IS state with a single electron in the e_g shell is strongly Jahn-Teller active, and an octahedron elongation at the Co^{3+} sites was interpreted as evidence for the IS state [137]. A study of the structural distortion with a four-circle diffractometer collecting many more reflections [138] does not support the IS state. Using this structural model, DFT finds a low-spin state [139]. Also the anisotropy of the magnetic susceptibility [127, 140] points to a low-spin state of Co^{3+} in the doping range $0.4 < x < 0.8$. In view of the large amount of conflicting interpretations a final conclusion about the spin-state near half doping seems not yet possible [141–146], in particular one may wonder whether simple local models can capture all the physics of $\text{La}_{2-x}\text{Sr}_x\text{CoO}_4$.

For the magnetic structure at half doping, there is no indication for a contribution of a magnetic Co^{3+} neither in the elastic scattering [21, 136–138] nor in the analysis of the magnetic excitations [138, 147, 148]. The magnetic structure in $\text{La}_{1.5}\text{Sr}_{0.5}\text{CoO}_4$ is not perfectly commensurate but the magnetic signal is slightly displaced already suggesting some charge inhomogeneity. Assuming non-magnetic Co^{3+} the magnetic structure arises from the exchange between two Co^{2+} in a distance of about 8 \AA , see Fig. 5 (b), whereas the interaction across the diagonals is frustrated. This splits the Co^{2+} -sites into two sets which can couple only through weaker inter-layer parameters. The magnetic structure may therefore become unstable against any minor modification lifting this degeneracy [21]. An introduction of an additional row of Co^{2+} or just polarizing magnetic sites in formal Co^{3+} rows lifts the degeneracy and

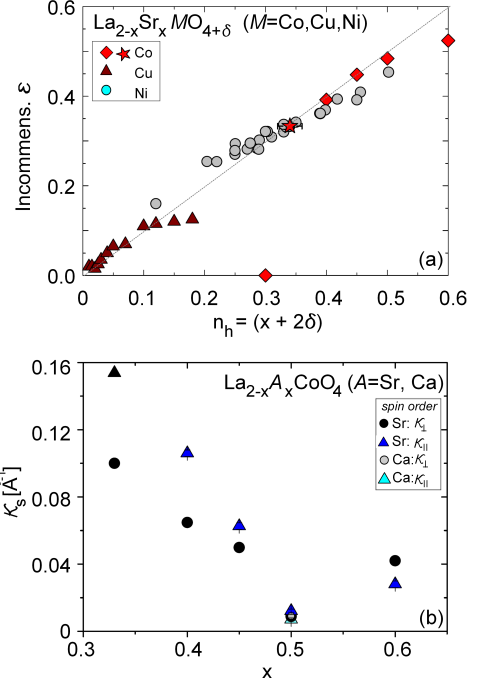


Figure 9: (a) Dependence of the charge incommensurability on the amount of doping in $\text{La}_{2-x}\text{Sr}_x\text{CoO}_4$ compared to nickelates and cobaltates; note that the values for the cuprates were scaled by a factor two to consider the different occupation of charges in the stripe (data taken from references [21, 152]). Inverse correlation lengths of the magnetic ordering in $\text{La}_{2-x}\text{Sr}_x\text{CoO}_4$ plotted against the amount of doping (b). Data taken from references [21, 152].

significantly strengthens the magnetic order, see Fig. 5 (c).

A single crystal with $x = 0.3$ doping was studied by polarized- and by unpolarized-neutron diffraction [21] revealing a significant suppression of the structural transition to $T_S = 227 \text{ K}$, see Fig. 7(a). The polarization analysis further reveals commensurate quasi-2D magnetic scattering around $\mathbf{Q} = (0.5, 0.5, 0)$ documenting that this material is still governed by the simple nn antiferromagnetic instability. Scanning in different directions with good resolution excludes that the broad signal actually arises from an incommensurate stripe phase corresponding to a doping of $x = 0.3$ [138]. The stability of the commensurate antiferromagnetism in $\text{La}_{2-x}\text{Sr}_x\text{CoO}_4$ is remarkable in view of the rapid suppression in cuprates and in nickelates. A possible explanation can be given in terms of the reduced mobility of charge carriers in layered cobaltates [121] which can be related not only with enhanced electron-phonon coupling but also with the spin states. Maignan et al. examined the possible electron transfer between a Co^{2+} and a neighboring Co^{3+} ion for different spin states in $\text{HoBaCo}_2\text{O}_{5.5}$, proposing the so-called spin-blockade mechanism [149]. For the case of a HS Co^{2+} neighboring a LS Co^{3+} , the e_g electrons of Co^{2+} cannot hop into the free e_g orbitals of Co^{3+} , since this would result in two unfavorable IS states and thus cost a high amount of energy. Electrons in a Co^{2+} HS and Co^{3+} LS lattice are thus effectively trapped explaining the higher resistivity of layered cobaltates. The observed reduction of the nn antiferromagnetic T_N in $\text{La}_{2-x}\text{Sr}_x\text{CoO}_4$ can be compared to the reduction of T_N in $\text{K}_2(\text{Co}_{1-x}\text{Mg}_x)\text{F}_4$ where a non-mobile non-magnetic impurity

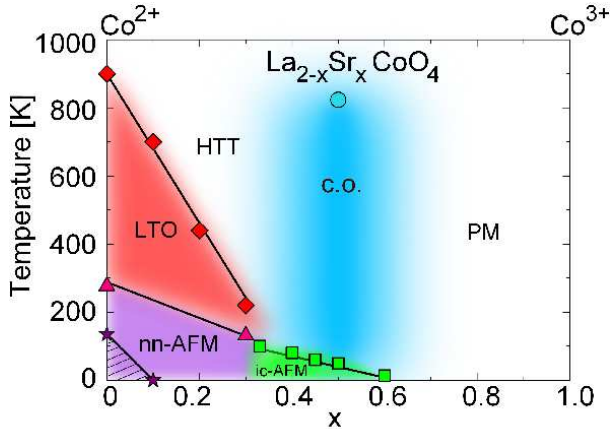


Figure 10: Phase diagram of $\text{La}_{2-x}\text{Sr}_x\text{CoO}_4$ indicating the structural phase transition into the LTO phase (red diamonds and line), the nn commensurate antiferromagnetism (magenta triangles) and the incommensurate magnetic stripe order (green squares); data are taken from references [21, 136, 137, 152].

is introduced [21, 138, 150]. The relative suppression of T_N is identical in both systems.

For slightly higher Sr content incommensurate scattering emerges similar to the case of the layered nickelates strongly suggesting a stripe arrangement of the diagonal type [Fig. 1(b) and Fig. 5(d)] [21, 152]. Figure 8 shows scans across the commensurate center of nn antiferromagnetism for $x = 0.4, 0.45, 0.5,$ and 0.6 (data taken from reference [21]). Figure 9(b) presents the doping dependence of the low temperature inverse correlation lengths and of the incommensurabilities found in these experiments. The magnetic scattering in $\text{La}_{2-x}\text{Sr}_x\text{CoO}_4$ remains quite broad and exhibits a pronounced in-plane anisotropy. The correlation along the modulation is much shorter than that perpendicular to it, which qualitatively agrees with the findings in the nickelates and the expectation for a solitonic stripe arrangement [83]. For the higher doping, the distance between two charges stripes is very short in this picture. Also the minimum of the inverse correlation length at $x = 0.5$, see Fig. 9, resembles the behavior in $\text{La}_{2-x}\text{Sr}_x\text{NiO}_4$, see Fig. 4, but in the nickelates, maximum stability appears already at $x = 1/3$. The most stable ordering in the cobaltates also manifests itself by larger correlation lengths and a higher integrated intensity. The magnetic phase is found to be more stable in $\text{La}_{1.5}\text{Ca}_{0.5}\text{CoO}_4$ due to the structural tilt distortion in this material and due to the reduced A-site disorder similar to the analysis of $\text{Re}_{1.67}\text{A}_{0.33}\text{NiO}_4$ [107].

The doping dependence of the incommensurability agrees almost perfectly with the expectation for the stripe ordering for $0.3 \leq x \leq 0.5$ and it naturally fits into the relations obtained for cuprates and nickelates suggesting the common mechanism in terms of charge segregation, see Fig. 9(a). Note that ε_{ch} has been scaled by a factor two in the case of the cuprates in order to take the different occupation in the charge stripe into account. Compared to cuprates and nickelates, stripe order in $\text{La}_{2-x}\text{Sr}_x\text{CoO}_4$ just starts at higher doping concentration. The incommensurability ε_{ch} for $\text{La}_{1.4}\text{Sr}_{0.6}\text{CoO}_4$ falls well below the expected value indicating the limit of the fully localized stripe

picture in the cobaltates.

There is, however, only weak evidence for incommensurate charge ordering in $\text{La}_{2-x}\text{Sr}_x\text{CoO}_4$ just a very diffuse signal was observed. Incommensurate magnetism has been reported also for higher doping but the underlying structure is not fully clarified [153].

The resulting phase diagram for $\text{La}_{2-x}\text{Sr}_x\text{CoO}_4$ closely resembles that for $\text{La}_{2-x}\text{Sr}_x\text{NiO}_4$, see Fig. 10 and Fig. 6. The structural distortion and the commensurate antiferromagnetism are suppressed with the doping. The slower suppression of the octahedron tilting can be attributed to the higher bond-length mismatch of the pure compound. The more robust nn antiferromagnetic structure has been proposed to result from the spin-blockade mechanism [21]. The crossover from commensurate to incommensurate antiferromagnetism appears again close to the full suppression of the structural distortion but still in the distorted phase. The second observation of an almost coincidence of the suppression of the structural distortion with the onset of stripe order eventually indicates some implication of the tilt disorder in the emergence of the stripe phase. The mixing of La and Sr on the same site induces significant disorder in $\text{La}_{2-x}\text{Sr}_x\text{CoO}_4$ that is further enhanced by the softening of the tilt instability around the structural transition. The influence of the La-Sr mixing on local tilt distortions was analyzed for $\text{La}_{2-x}\text{Sr}_x\text{CuO}_4$ [151] and should be even stronger in the case of the cobaltates due to the larger amount of Sr doping. Due to the disorder, one may not expect a sharp structural transition neither as function of doping nor as function of temperature, but strong local distortions should exist on both sides of the transition. These might favor the stripe order and further destabilize the commensurate antiferromagnetism. The magnetic transition temperatures presented in Fig. 10 have to be regarded with caution, because they most likely are subject to severe time-scale issues. The data in reference [21] were measured on a cold instrument yielding a characteristic time scale of a few ps, any fluctuation slower than this will appear as an elastic signal in this experiment. The decrease of magnetic transition temperatures appears to be almost linear in the doping, even across the transition from commensurate to incommensurate magnetism, which may reflect and thus support the continuous suppression of magnetic moments with doping as expected for LS Co^{3+} .

Magnetic excitations in $\text{La}_{2-x}\text{Sr}_x\text{CoO}_4$ were studied for pure La_2CoO_4 [154], for half-doped $\text{La}_{1.5}\text{Sr}_{0.5}\text{CoO}_4$ [138, 147, 148] and more recently also for $\text{La}_{1.67}\text{Sr}_{0.33}\text{CoO}_4$ [152]. The magnon dispersion in the pure and in the half-doped material can be well described by linear spin-wave theory and thus allows one to determine the magnetic interaction between two neighboring Co^{2+} moments J_m and that between two Co^{2+} moments connected by an intermediate non-magnetic Co^{3+} , J'' see Fig. 5 (d) [152]. In $\text{La}_{1.67}\text{Sr}_{0.33}\text{CoO}_4$ Boothroyd et al. find magnetic stripe ordering very similar to the stable state in $\text{La}_{1.67}\text{Sr}_{0.33}\text{NiO}_4$ [152] but with very short in-plane correlation lengths of only $\xi_{\parallel}^S = 6.5 \text{ \AA}$ and $\xi_{\perp}^S = 10 \text{ \AA}$ parallel and perpendicular to the stripe modulation, respectively (note that these directions are perpendicular and parallel to the stripes, respectively). Most interestingly they find the magnon dispersion to exhibit an hourglass-

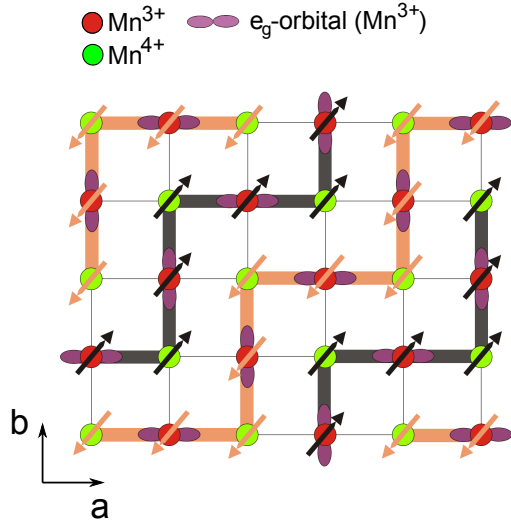


Figure 11: Schematic arrangement of the charge, orbital, and magnetic ordering in half doped manganites, a single layer is shown. In the Goodenough model charges exhibit checkerboard order with orbital order occurring on the Mn^{3+} $3d^4$ sites with a single e_g electron. The aligned e_g orbital mediates a strong ferromagnetic interaction resulting in zigzag ferromagnetic chains that are antiferromagnetically stacked.

shaped dispersion, like it has been observed for many cuprates materials [14–18]. This strengthens the interpretation, that fluctuating stripes are the proper basis to describe the magnetic excitation in the cuprates in contrast to purely itinerant models [19]. Phonon studies have not been reported for layered cobaltates, but one may expect similar anomalies as in the case of the nickelates [84, 85].

4. Incommensurate order of charges, spins and orbitals in layered manganites

The colossal magnetoresistance (CMR) reported for several manganese oxides [155, 156] stimulated comprehensive studies in experiment and theory, since this phenomenon promised a high potential for applications. The Zener double-exchange mechanism can only explain a small part of the drop of resistivity by several orders of magnitude that is implied by only moderate external magnetic fields [157]. The essential part of the CMR effect arises from the competition between insulating antiferromagnetic states and a ferromagnetic metallic phase. By application of a magnetic field one induces an insulator-metal transition into the ferromagnetic state which is accompanied by the loss of resistivity [155, 158]. Understanding the CMR thus means understanding the interplay of the different phases including their segregation [159–163] and, most importantly, understanding the character of the insulating phases. These insulating phases exhibit charge and orbital ordering accompanied by antiferromagnetic ordering at low temperatures, but the phase diagrams of the manganites exhibit a remarkable variety of such charge and orbital ordered phases [156]. In spite of comprehensive experimental and theoretical efforts the knowledge about the insulating state is still limited and controversial proposals have been made even for fundamental questions like

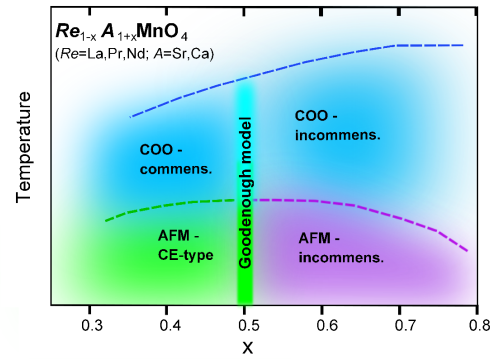


Figure 12: Phase diagram of $\text{La}_{1-x}\text{Sr}_x\text{MnO}_4$ indicating the charge, orbital and magnetic ordering near half doping; note that phase diagrams of various perovskite phases are very similar. Underdoping with respect to half doping results in an almost commensurate order very similar to the Goodenough model described in Fig. 11, whereas overdoping immediately implies incommensurate modulations that perfectly follow the amount of doping.

site [164–166] or bond centering [167] of the charge order. The role of the stripe order for high-temperature superconductivity can still be questioned, but there is no doubt that charge-ordered phases are essential for the CMR effect.

The most stable and best characterized charge and orbital ordered phase occurs at half doping either in the perovskite materials, $(\text{Re}_{1-x}\text{A}_x\text{MnO}_3$ with $\text{Re} = \text{La}, \text{Y}$ or a rare earth and A in most cases an earth alkali) or in single- or double-layered compounds. The model proposed very early for $\text{La}_{0.5}\text{Ca}_{0.5}\text{MnO}_3$ consists of a checkerboard ordering of the charges accompanied by orbital ordering at the Mn^{3+} site and is called Goodenough model, it is depicted in Fig. 11 [165, 166]. Mn^{3+} ion with $3d^4$ configuration and a single electron in the e_g shell is strongly Jahn-Teller active and the aligning of the orbital mediates a strong ferromagnetic interaction with the neighboring Mn^{4+} moments (corresponding to a $3d^3$ configuration). In Fig. 11, we show a schematic picture of this charge, orbital, and magnetic arrangement for a single MnO_2 layer. Due to strong structural distortions even the perovskite materials exhibit some layered character with the planes of charge and orbital order always aligning along the ab planes (in space group Pbnm). Single-layered manganites $\text{La}_{1-x}\text{Sr}_x\text{MnO}_4$ [168] do not exhibit the CMR effect unless very high magnetic fields are applied and even then only bad metallic properties are observed [169]. However, these materials are much better suited for any scattering studies of charge and orbital order due to the absence of the complex twinning and due to the availability of large single crystals [170]. Half-doped $\text{La}_{0.5}\text{Sr}_{1.5}\text{MnO}_4$ has been studied by many different techniques [171–179] and the charge and orbital ordered state of this material can be considered as the best characterized one amongst all manganites. It is well established for this material, that the Goodenough model is the appropriate one to describe the charge and orbital order [178, 179] but only qualitatively. The modulation of the electronic charge is far below the integer value but the orbital polarization at the nominal Mn^{3+} site is nearly complete [177]. The small modulation of

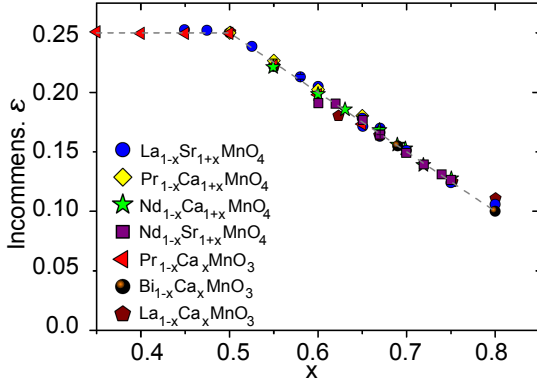


Figure 13: Dependence of the orbital modulation on the doping across the half-doped composition for various manganite systems. Below half doping the order stays almost commensurate, but above half doping the orbital incommensurability perfectly follows the amount of excess Mn^{4+} with respect to half doping, $\varepsilon_{oo} = 0.25 - \frac{\Delta x}{2}$. This strict rule underlines the dominant role of the orbital ordering in the stripe phases in overdoped manganites. Data were taken from references [22, 176, 211] for $\text{La}_{1-x}\text{Sr}_{1+x}\text{MnO}_4$, [194, 210] for $\text{Pr}_{1-x}\text{Ca}_{1+x}\text{MnO}_4$, [195] for $\text{Nd}_{1-x}\text{Ca}_{1+x}\text{MnO}_4$, [188, 212] for $\text{Nd}_{1-x}\text{Sr}_{1+x}\text{MnO}_4$, [194] for $\text{Pr}_{1-x}\text{Ca}_x\text{MnO}_3$, [203] for $\text{Bi}_{1-x}\text{Ca}_x\text{MnO}_3$, and [24] for $\text{La}_{1-x}\text{Ca}_x\text{MnO}_3$.

the electronic charge is also found in perovskite materials [180–182] so that it can be considered as representative for charge ordered states in manganites. Four different types of superstructure reflections can be identified in half-doped $\text{La}_{0.5}\text{Sr}_{1.5}\text{MnO}_4$ [22, 182, 184]. Neglecting the inter-layer coupling, charge order causes weak super structure reflections at $\mathbf{k}_{\text{ch}} = \pm(0.5, 0.5)$. The orbital order can be considered as the main element of the structural distortion in $\text{La}_{0.5}\text{Sr}_{1.5}\text{MnO}_4$ [173, 177] and is associated with the strongest nuclear superstructure peaks appearing at $\mathbf{k}_{oo} = \pm(0.25, 0.25)$. The orbital arrangement can be considered as stacking of rows of parallel orbitals with a 90° rotation of the orbital order in neighboring orbital rows. The magnetic order is described by two propagation vectors $\mathbf{k}_{\text{Mn}^{3+}} = \pm(0.25, -0.25)$ and $\mathbf{k}_{\text{Mn}^{4+}} = \pm(0.5, 0.0)$ referring to the nominal Mn^{3+} and Mn^{4+} spins, respectively.

The phase diagram of $\text{La}_{1-x}\text{Sr}_{1+x}\text{MnO}_4$ is quite different to those discussed in the previous sections, as we start for $x = 0$ with LaSrMnO_4 which only possesses Mn^{3+} sites and is thus comparable to LaMnO_3 . The transport, magnetic [168] and structural [183] properties of this system are well known. The pure material exhibits an antiferromagnetic ordering with the moments aligning along the c direction. This magnetic structure is coupled with an e_g orbital alignment along the c direction [176, 183]. Upon further increase of the Sr content the antiferromagnetism is suppressed and orbitals flop into the planes as is indicated in Fig. 11 for $x = 0.5$ [183].

Evidence for an incommensurate ordering of charges and orbitals has been found in electron diffraction experiments shortly after the revival of interest in $\text{La}_{1-x}\text{Ca}_x\text{MnO}_3$ due to the discovery of the CMR effect [23, 24, 185]. The first experiments were interpreted in terms of simple charge ordering and revealed a linear relationship between the incommensurability and the electronic doping, which should be considered as the finger print of a stripe phase [23, 24, 185]. In

our notation, the strongest nuclear superstructure reflections appear at $\varepsilon_{oo} = (\varepsilon_{oo}, \varepsilon_{oo}, q_l)$ shifted from a fundamental Bragg peak and arise from orbital ordering [172, 179]. The relation $\varepsilon_{oo} = 0.5 - \frac{x}{2} = 0.25 - \frac{\Delta x}{2}$ with Δx the amount of overdoping, $\Delta x = x - 0.5$, is perfectly fulfilled in many different manganites systems including perovskite and layered phases [22–24, 172, 176, 194, 194, 203, 210–212], see Fig. 13. There is a striking asymmetry between over- and underdoping with respect to half doping: Slightly below $x = 0.5$ the orbital order appears at or close to the commensurate quarter-indexed position, whereas the linear relation is immediately fulfilled for even small overdoping.

The perfect confirmation of the $\varepsilon_{oo} = 0.25 - \frac{\Delta x}{2}$ rule for so many different manganites systems with perovskite and layered structure is remarkable [22–24, 172, 176, 194, 194, 203, 210–212], see Fig. 13. For overdoping with respect to halfdoping, the linear relation is almost perfectly fulfilled for $\text{La}_{1-x}\text{Sr}_{1+x}\text{MnO}_4$ [22, 176, 211], $\text{Pr}_{1-x}\text{Ca}_{1+x}\text{MnO}_4$ [194, 210], $\text{Nd}_{1-x}\text{Ca}_{1+x}\text{MnO}_4$ [195], $\text{Nd}_{1-x}\text{Sr}_{1+x}\text{MnO}_4$ [188, 212], $\text{Pr}_{1-x}\text{Ca}_x\text{MnO}_3$ [194], $\text{Bi}_{1-x}\text{Ca}_x\text{MnO}_3$ [203], $\text{Bi}_{1-x}\text{Sr}_x\text{MnO}_3$ [200], and $\text{La}_{1-x}\text{Ca}_x\text{MnO}_3$ [24]. The underlying orbital order certainly is the key element to understand the stripe phases in overdoped manganites. The law can be easily explained with the Wigner model: There is strong tendency to form diagonal rows of parallel Mn^{3+} orbitals with the distance between them given by the amount of excess Mn^{4+} . A further factor two in the incommensurability arises from the 90° rotation of the orbitals in neighboring orbital stripes. As for the CE-type ordering at half doping, one may then ask whether this orbital ordering has a purely structural or a partially magnetic mechanism [204–209]. The ordering in a single orbital stripe implies a strong ferromagnetic interaction of the central Mn^{3+} with the two Mn^{4+} neighboring moments along the occupied e_g orbital, in addition the stacking of these ferromagnetic trimers is antiferromagnetic.

We wish to emphasize, however, that the stripe phase in overdoped manganites is fundamentally different from all those discussed above, because it is already a charge and orbitally ordered state which becomes incommensurately modulated by the variation of doping. The asymmetry is most likely related with the fact that Mn^{3+} can take the place of Mn^{4+} by flopping the orbital perpendicular to the plane [186].

In spite of strong efforts [23–25, 162, 176, 177, 187–203] the incommensurate stripe-like phases for overdoping are insufficiently understood and essential questions about the nature of the electronic arrangement and about the homogeneity of the modulation remain matter of controversy. The observation of the superstructure reflections in the diagonal direction indicates orbital rows running along the diagonals. The excess rows of Mn^{4+} with respect to half doping run along the diagonals as well. However, there are different possibilities to arrange the orbital rows. In the so-called Wigner model the rows with parallel Mn^{3+} orbitals arrange as far as possible, whereas high-resolution transmission electron microscopy suggests that two such Mn^{3+} rows together with a shared Mn^{4+} line form a bi-stripe [25]. The bi-stripe can be identified with a single "zig" in the zigzag ferromagnetic chains of the CE-type structure, see

Fig. 11, at half-doping; this model suggests a strong stability of the bi-stripe local distortion. Also a double stripe of two directly neighboring Mn^{3+} rows was proposed [200].

Numerous electron, x-ray and neutron diffraction experiments studied the stripe phases in various overdoped manganites, however, without reaching a clear conclusion [176, 177, 187–189, 192, 193, 201, 202]. Concerning the question about bi-stripe versus Wigner model, the larger part of the experiments favor the Wigner model [187, 198, 199, 203] for the perovskites compounds, whereas experiments on double-layer manganites were interpreted in terms of the bi-stripe model [192, 193] but a clear experimental proof for one of the two scenarios is still missing. Note, however, that only for doping above $x = 0.6$ there is a difference between the two models as otherwise bi-stripes form also in the Wigner model.

Both a soliton lattice [22, 162, 190, 191, 197] and a homogeneous charge-density wave [189, 196] have been proposed to explain the incommensurabilities generating again strong controversy. However, the recent observation of remarkably strong second-order harmonics of the orbital ordering reflection as well as NMR experiments give strong support for a solitonic arrangement of well defined stripes of excess Mn^{4+} [22, 197], whereas the argumentation in reference [189] can be questioned.

The interplay between the orbital order and the magnetism is well studied for $\text{La}_{0.5}\text{Sr}_{1.5}\text{MnO}_4$ [178, 179]. Both phenomena are closely coupled, because the e_g orbital always implies a strong directed ferromagnetic interaction. Therefore, it is not easy to analyze which instability is driving and which is following [204–209]. The sequence of the magnetic correlations with isotropic short-range ferromagnetic correlations above T_{co} and anisotropic ferromagnetic and antiferromagnetic correlations for $T_N < T < T_{co}$ and long-range CE-type ordering below T_N is obtained in several analyzes [206, 208, 209]. The fact that the orbital scattering coexists at high temperature $T > T_{co}$ with ferromagnetic short-range order suggests strong electron-lattice coupling driving the orbital ordering. This conclusion is further corroborated by measurements on overdoped $\text{La}_{0.42}\text{Sr}_{1.58}\text{MnO}_4$ [22], $\text{Pr}_{0.33}\text{Ca}_{1.67}\text{MnO}_4$, and $\text{Nd}_{0.33}\text{Sr}_{1.67}\text{MnO}_4$ [210] in which incommensurate orbital scattering coexists with ferromagnetic correlations without any measurable change in the position.

Due to the complex twinning in the perovskites and due to the complex arrangement of the orbital, charge and spin order in overdoped manganites, a full model of the different order parameters could not be developed for the perovskite phases. For slightly overdoped layered manganites, $\text{La}_{0.42}\text{Sr}_{1.58}\text{MnO}_4$ and $\text{La}_{0.45}\text{Sr}_{1.55}\text{MnO}_4$, a full mapping of the neutron scattering was measured as function of temperature and allowed establishing a consistent model [22]. Fig. 14 shows the low temperature map together with a model for the stripe ordering in this material. The mapping as well as comprehensive additional neutron diffraction experiments indicate that the sharp superstructure peaks in $\text{La}_{0.5}\text{Sr}_{1.5}\text{MnO}_4$ become incommensurately displaced and broadened in $\text{La}_{0.42}\text{Sr}_{1.58}\text{MnO}_4$. Three incommensurate and one commensurate superstructure can be identified. Charge order reflections are found at $\mathbf{Q} = (1.5 \pm \varepsilon_{ch}, 1.5 \pm \varepsilon_{ch}, 0)$ with $\varepsilon_{ch} = 0.080(3)$. The orbital satellites are centered closer

to the Bragg-reflection, for example $\mathbf{Q} = (0, 2, 0)$, in diagonal direction in perfect agreement with data for layered and perovskite manganites, $\mathbf{k}_{oo} = (0.25 - \Delta\varepsilon_{oo}, 0.25 - \Delta\varepsilon_{oo}, 0)$. Neither the charge nor the orbital scattering exhibit any measurable temperature dependency concerning their positions, and the incommensurabilities of charge and orbital scattering differ precisely by a factor 2, ($\Delta\varepsilon_{oo} = 0.039(2) = \frac{1}{2}\varepsilon_{ch}$).

The magnetic scattering associated with the Mn^{3+} is also incommensurate in $\text{La}_{1-x}\text{Sr}_{1+x}\text{MnO}_4$ with x slightly above 0.5. The modulation is transverse with respect to the quarter-indexed peaks in $\text{La}_{0.5}\text{Sr}_{1.5}\text{MnO}_4$, $\mathbf{k}_{\text{Mn}^{3+}} = (0.25 - \varepsilon_{\text{Mn}^{3+}}, 0.25 + \varepsilon_{\text{Mn}^{3+}}, 0)$ [22], and the modulation length exactly agrees with the two nuclear ones: $\varepsilon_{\text{Mn}^{3+}} = 0.037(2) = \Delta\varepsilon_{oo} = \frac{1}{2}\varepsilon_{ch}$. In contrast to these three incommensurate order parameters, the magnetic scattering associated with the ordering of Mn^{4+} spins remains commensurate.

The close coupling of the structural and magnetic superstructures corroborates the stripe-like arrangement previously deduced from the structural distortions only. Since all modulations point along the diagonals, the excess Mn^{4+} must align along the diagonals thereby interrupting the ferromagnetic zigzag chains of the CE-type structure which run along the perpendicular diagonals. A model for the charge orbital and stripe order in $\text{La}_{0.42}\text{Sr}_{1.58}\text{MnO}_4$ is presented in Fig. 14. For $x = 0.6$ a simple commensurate model consists of a bi-stripe combined with a double Mn^{4+} stripe. This pattern has a width of five diagonal rows. For $x = 0.57 \sim \frac{4}{7}$ a similar commensurate model is constructed with a width of seven rows. In order to obtain an incommensurate arrangement corresponding to the doping of $x = 0.58$, the five- and seven-rows models can be combined in the appropriate ratio as it is illustrated Fig. 14. This solitonic arrangement of stripes gives a perfect description of all scattering intensities in $\text{La}_{0.42}\text{Sr}_{1.58}\text{MnO}_4$ [22]. In particular the simple Fourier transform of large supercells describes the diffuse shape of the magnetic scattering which exhibits characteristic tails along the diagonals. This shape can be taken as further evidence for the solitonic stripe arrangement [83].

Increasing the doping beyond $x = 0.6$ one may distinguish between the Wigner and the bi-stripe arrangement of the orbital ordering. The perfect relation between the incommensurability and the doping, which shows no anomaly near $x = 0.6$, indicates that the orbital ordering continues smoothly across this value. Clearly, orbital ordering is the main element to describe the complex ordered states in overdoped manganites. Although we still lack a full experimental proof, there is stronger support for the Wigner model in perovskite and single-layered manganites in the doping rang $0.6 < x < 0.8$ [187, 198, 199, 203]. Mapping the different superstructure intensities in $\text{Nd}_{0.33}\text{Sr}_{1.67}\text{MnO}_4$ and in $\text{Pr}_{0.33}\text{Ca}_{1.67}\text{MnO}_4$ with the flatcone neutron detector, we also find clear evidence for the Wigner model in the single-layered manganites [210]. Orbital ordering in heavily overdoped manganites consists of diagonal stripes of Mn^{3+} with parallel alignment of the e_g -orbitals. These orbital rows result in three Mn-sites thick blocks with strong magnetic coupling, see Fig. 15. The two Mn^{4+} moments neighboring the Mn^{3+} are ferromagnetically coupled and there is an antiferromagnetic coupling in between two such trimers. However, the

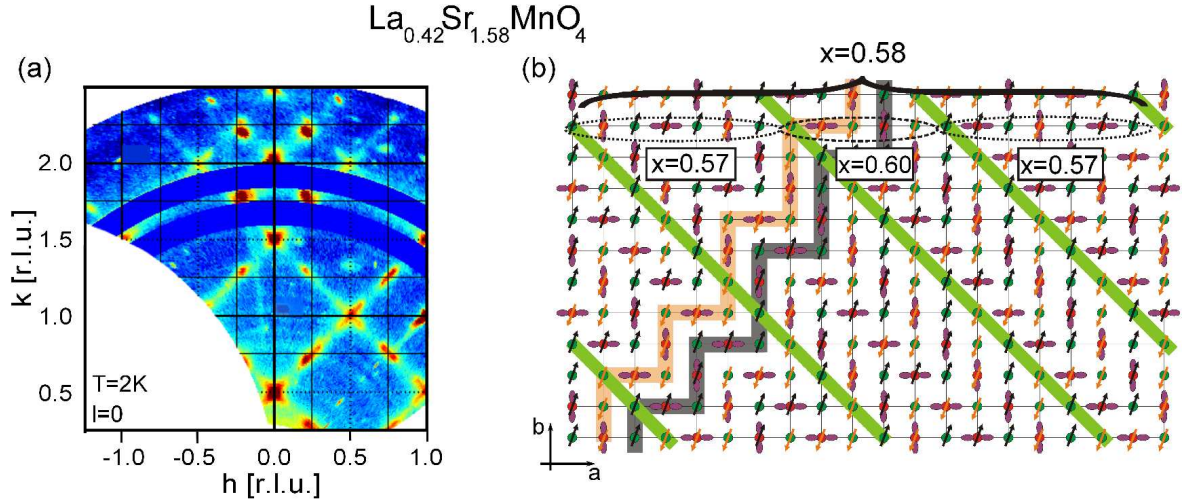


Figure 14: Distribution of structural and magnetic scattering in the $(h,k,0)$ plane for $\text{La}_{0.42}\text{Sr}_{1.58}\text{MnO}_4$ arising from incommensurate ordering of charge, orbital and magnetic ordering of Mn^{3+} (a). Sketch of charge, orbital and spin order for $\text{La}_{0.42}\text{Sr}_{1.58}\text{MnO}_4$ (b). Red circles represent Mn^{3+} and green circles Mn^{4+} . A single domain of zigzag chains propagating in $[110]$ direction is shown. The excess lines of Mn^{4+} are displayed on a green background. A local variation of stripe distances is needed to account for the real charge concentration (data taken from references [22, 24, 176, 194, 195, 210]).

coupling between two stripes is very weak due to frustration, see Fig. 15. The magnetic scattering is quite different to that appearing at lower overdoping. Instead of incommensurate Mn^{3+} and commensurate Mn^{4+} magnetic scattering, one finds incommensurate signals around the Mn^{4+} position and commensurate quarter-indexed scattering for $x = 2/3$. The fact that the incommensurate magnetic modulations change between $x = 0.58$ and 0.67 without any anomaly in the orbital ordering, see Fig. 13, clearly indicates that the orbital pattern is independent of the magnetic arrangement. The orbital pattern is mainly associated with the magnetic coupling within the stripe whereas the inter-stripe coupling represents a much smaller energy scale, see below.

There is also evidence for self-organized charge, orbital and magnetic ordering in some underdoped manganites [213], but different propagation vectors seem to coexist and a conclusive model of all types of order for such materials is still lacking.

There are numerous studies on the magnetic excitations focussing on the metallic ferromagnetic phases, see the discussion in references [214, 215], and on the low-doping [216] concentration range, but the magnon dispersion in the CE-type phase at half doping has been reported only recently [178, 179, 184] due to the difficulties to analyze this complex order with twinned crystals. In the CE-type phase, the strongest magnetic coupling is found between a Mn^{3+} and Mn^{4+} moment coupled through the ordered e_g orbital, like it is expected in the Goodenough model. This dominating magnetic interaction gives rise to strong anisotropy in the spin-wave dispersion, which is much steeper along the ferromagnetic zigzag chains [178, 179, 184]. Very recently, the spin-wave dispersion has also been studied for overdoped manganites which exhibit a stripe arrangement of orbitals and charges. Most interestingly, $\text{Nd}_{0.33}\text{Sr}_{1.67}\text{MnO}_4$ and $\text{Pr}_{0.33}\text{Ca}_{1.67}\text{MnO}_4$ exhibit a hourglass dispersion very similar to those reported for the cuprates [14–18] and for $\text{La}_{1.67}\text{Sr}_{0.33}\text{CoO}_4$ [152]. $\text{Pr}_{0.33}\text{Ca}_{1.67}\text{MnO}_4$ ex-

hibits a better defined magnetic ordering at low temperature due to structural distortions that the smaller A-site ions imply, and due to the smaller internal disorder. Note that Pr and Ca possess similar ionic radii, whereas those of La and Sr or of Nd and Sr differ considerably. The longer correlation lengths in $\text{Pr}_{0.33}\text{Ca}_{1.67}\text{MnO}_4$ offer an additional insight in the causes for the hourglass-shaped dispersion. At low temperature, when the correlation lengths are longer, one finds the outwards dispersing branches but these become suppressed upon heating when correlation lengths diminish. $\text{Nd}_{0.33}\text{Sr}_{1.67}\text{MnO}_4$ exhibits short correlation lengths even at low temperature and no indication for the outwards bending branches [210]. Short magnetic correlation lengths appear to be a necessary condition for the insulating stripe phases to exhibit an hourglass dispersion. The short correlation lengths in $x = 2/3$ doped manganites are a consequence of the frustrated coupling between the magnetically well determined orbital stripes, see Fig. 15. In this view these manganites closely resemble the cuprates, with weak coupling of the antiferromagnetic blocks across the charge stripes, and also the layered cobaltate, where the non-magnetic Co^{3+} sites reduce the coupling across the charge stripes.

5. Conclusions

Overwhelming evidence for stripe-like arrangement of charges, magnetic moments and orbital degrees of freedom has been found in several layered non-cuprates transition-metal oxides. Incommensurate ordering of charges, orbitals, and magnetic moments should be considered as the rule and not as the exception in transition-metal oxides. The main difference with the stripes phases discussed for the cuprates concerns the insulating properties of the non-cuprates compounds, which are supposed to arise from a stronger electron-lattice interaction. There is reasonable evidence that the stripe patterns with solitonic and local moment character depicted in Fig. 1 and 14 are

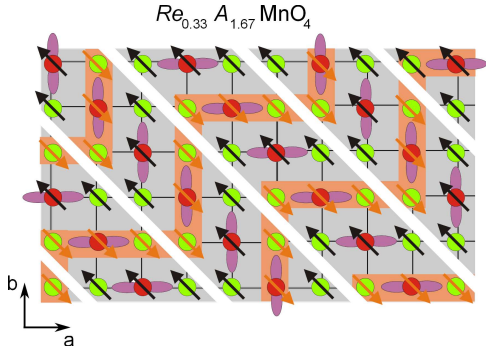


Figure 15: Schematic picture of the charge orbital and magnetic ordering in $x = 2/3$ doped layered manganites, $\text{Nd}_{0.33}\text{Sr}_{1.67}\text{MnO}_4$ and $\text{Pr}_{0.33}\text{Ca}_{1.67}\text{MnO}_4$; the main structural element consists in rows of Mn^{3+} sites with parallel e_g orbitals, that lead to a magnetically well defined block of three Mn sites width. The magnetic coupling between these orbital stripes, however, is frustrated.

better suited to describe these insulating phases than a coupled CDW/SDW scenario, whereas this question still is an open issue in the cuprates.

In none of the systems described here, one finds an integer modulation of the charge at the metal ion site [26, 177, 180–182]. Like in other charge ordered transition-metal oxides, e.g. Fe_3O_4 , a purely ionic model is insufficient to describe the charge and orbital ordering even for these insulating materials. Due to covalency and hybridization with the oxygen orbitals a larger part of the charge modulation in all these materials occurs on the bonds surrounding the metal ion, but the ordering seems to be still centered at the metal site in the layered nickelates and manganites. This spread charge modulation, however, does not contradict the local character of the stripe phase depicted.

The phase diagrams of $\text{La}_{2-x}\text{Sr}_x\text{MO}_4$ with $M = \text{Cu}, \text{Ni}$ or Co are remarkably similar. All the pure materials exhibit a structural phase transition characterized by octahedron tilting that is followed by a second structural transition due to a change of the tilt axis in the case of Ni and Co. This structural instability is perfectly explained through the bond-length mismatch, which is partially released by the doping due to the larger ionic radius of Sr and due to the smaller induced radius at the oxidized metal ion. Due to the stronger starting mismatch in La_2CoO_4 it takes a larger amount of doping to fully suppress the structural distortion in $\text{La}_{2-x}\text{Sr}_x\text{CoO}_4$ compared to $\text{La}_{2-x}\text{Sr}_x\text{NiO}_4$ and $\text{La}_{2-x}\text{Sr}_x\text{CuO}_4$. Also the nn antiferromagnetism is suppressed with the doping in all three systems, but the amount of doping needed for full suppression does not correlate with the T_N of the parent compound. The mobility of the induced holes seems to be decisive for the suppression of the nn antiferromagnetism, occurring at $\sim 2\%$, $\sim 17.5\%$ and $\sim 30\%$ in cuprates, nickelates and cobaltates, respectively. All three systems show evidence for magnetic stripe ordering appearing next to the commensurate phases. In nickelates and cobaltates the onset of stripe order almost coincides with the suppression of the tilt distortion. Due to the intrinsic disorder induced by the doping the structural transition is not well-defined in $\text{La}_{2-x}\text{Sr}_x\text{NiO}_4$ and in $\text{La}_{2-x}\text{Sr}_x\text{CoO}_4$ and the enhanced local variation of the tilt angles in the vicinity of the transition can help stabilizing

the stripe order or destabilizing the nn commensurate antiferromagnetic order.

The relationship between the structural and magnetic modulation and the amount of charge doping, $\varepsilon_{ch} \propto n_h$, can be considered as the characteristic finger print of a stripe phase with local charge and magnetic character, as a CDW/SDW instability arising from Fermi-surface features can adopt any value. Ti-doped Sr_2RuO_4 is an example of an isostructural metallic compound that exhibits incommensurate magnetic ordering arising from a nesting instability [217, 218] which should be considered as a homogenous SDW. The $\varepsilon_{ch} \propto n_h$ relationship is better fulfilled in the insulating materials than in the cuprates, although there still are deviations. In the nickelates the very stable order at $1/3$ doping deforms the $\varepsilon_{ch}(x)$ relation in particular at higher temperatures. Similar effects are found in the layered cobaltates for $x > 0.5$ and in the manganites for $x < 0.5$, associated with an asymmetry of the phase diagram around the stable phase at half doping. Self-doping and non-local effects thus are already present in these insulating stripe phases: at both sides of the $1/3$ doping in the case of nickelates, whereas cobaltates and manganites tend to assimilate the stable ordering only at one unfavorable side.

In the manganites, clear evidence for stripe ordering with localized character is found in materials that are overdoped with respect to half-doping. These phases and the resulting phase diagrams are different, because it is an already charge and orbital ordered state that becomes further modulated or interrupted by rows of additional charges. The orbital ordering clearly constitutes the most important element to understand the complex ordering in the manganites. For large overdoping Mn^{3+} sites and their e_g orbitals form stripes, and the distance between them is perfectly well described by the amount of doping (assuming a Wigner model). The perfectly fulfilled $\varepsilon = 0.25 - \frac{\Delta x}{2}$ relation in many different families of overdoped manganites demonstrates the outstanding stability of the orbital ordering with the strong tendency to form an orbital stripe which then mediates the magnetic coupling. There are indications in the manganites that the orbital and the incommensurate magnetic ordering are decoupled.

The analysis of the magnetic excitations in the stripe-ordered insulating phases is most interesting with respect to the hourglass-shaped dispersion reported for the cuprates. Stripe ordered nickelates do not exhibit such a dispersion due to the very stable order at $1/3$ doping with a strong interaction across the charge stripes. However $\text{La}_{1.67}\text{Sr}_{0.33}\text{CoO}_4$, $\text{Nd}_{0.33}\text{Sr}_{1.67}\text{MnO}_4$, and $\text{Pr}_{0.33}\text{Ca}_{1.67}\text{MnO}_4$ were recently shown to exhibit the characteristic features of the hourglass dispersion. The hourglass dispersion differs from that predicted by linear spin-wave theory mostly by the suppression of the outwards dispersing branches. This feature was shown to be caused by the reduction of the magnetic correlation lengths to the order of the distance between the charge stripes. The common element of the metallic cuprates and the insulating cobaltates and manganites seems to consist in the local magnetic structure arising from well defined magnetic stripes that remain loosely coupled. In the cuprates and in the cobaltates these stripes consist of the nn antiferromagnetic regions in between two charge stripes, see

Fig. 1(b) and (c), whereas they are formed through the orbital ordering in the manganites, see Fig. 15. In all three cases the magnetic interaction between these stripes is extremely weak reminding a magnetically smectic phase [8]. Insulating stripe patterns with local character thus yield the same hourglass dispersion as the cuprates, however this does not exclude a more itinerant model needed to fully understand the cuprates.

This work was supported by the Deutsche Forschungsgemeinschaft through Sonderforschungsbereich 608. We acknowledge long collaboration and numerous stimulating discussions with M. Cwik, A.C. Komarek, T. Lorenz, C. Schüssler-Langeheine, O.J. Schumann, D. Senff, Y. Sidis, P. Steffens, and J. Tranquada.

References

- [1] J.M. Tranquada, B. J. Sternlieb, J. D. Axe, Y. Nakamura, and S. Uchida, *Nature (London)* **375**, 561 (1995).
- [2] D. Poilblanc and T.M. Rice *Phys. Rev. B* **39**, 9749 (1989).
- [3] J. Zaanen and O. Gunnarson, *Phys. Rev. B* **40**, 7391 (1989).
- [4] H.J. Schulz, *Phys. Rev. Lett.* **64**, 1445 (1990).
- [5] H.J. Schulz, *J. Phys.* **50**, 2833 (1989).
- [6] K. Machida, *Physica C* **158**, 192 (1989).
- [7] V.J. Emery and S.A. Kivelson, *Physica C* **209C**, 597 (1993).
- [8] S.A. Kivelson, I. P. Bindloss, E. Fradkin, V. Oganesyan, J. M. Tranquada, A. Kapitulnik and C. Howald, *Rev. Mod. Phys.* **75**, 1201 (2003).
- [9] M. K. Crawford, R. L. Harlow, E. M. McCarron, W. E. Farneth, J. D. Axe, H. Chou, and Q. Huang, *Phys. Rev. B* **44**, 7749 (1991).
- [10] B. Büchner, M. Cramm, M. Braden, W. Braunsch, O. Hoffels, W. Schnelle, R. Müller, A. Freimuth, W. Schlabit, G. Heger, D.I. Khomskii, and D. Wohlleben, *Europhys. Lett.* **21**, 953 (1993).
- [11] N. Ichikawa, S. Uchida, J. M. Tranquada, T. Niemöller, P. M. Gehring, S.-H. Lee, and J. R. Schneider, *Phys. Rev. Lett.* **85**, 1738 (2000).
- [12] J. M. Tranquada, J. D. Axe, N. Ichikawa, A. R. Moodenbaugh, Y. Nakamura, and S. Uchida, *Phys. Rev. Lett.* **78**, 338 (1997).
- [13] M. Arai, T. Nishijima, Y. Endoh, T. Egami, S. Tajima, K. Tomimoto, Y. Shiohara, M. Takahashi, A. Garrett, and S. M. Bennington, *Phys. Rev. Lett.* **83**, 608 (1999).
- [14] J. M. Tranquada, H. Woo, T. G. Perring, H. Goka, G. D. Gu, G. Xu, M. Fujita, and K. Yamada, *Nature* **429**, 534 (2004).
- [15] S. M. Hayden, H. A. Mook, P. Dai, T. G. Perring, and F. Dogan, *Nature* **429**, 531 (2004).
- [16] V. Hinkov, S. Pailhès, P. Bourges, Y. Sidis, A. Ivanov, A. Kulakov, C. T. Lin, D. P. Chen, C. Bernhard, and B. Keimer, *Nat. Phys.* **3**, 780 (2007).
- [17] O. J. Lipscombe, S. M. Hayden, B. Vignolle, D. F. McMorrow, and T. G. Perring, *Phys. Rev. Lett.* **99**, 067002 (2007).
- [18] Guangyong Xu, J. M. Tranquada, T. G. Perring, G. D. Gu, M. Fujita, and K. Yamada, *Phys. Rev. B* **76**, 014508 (2007).
- [19] M. Eschrig, *Adv. Phys.* **55**, 47 (2006).
- [20] J. M. Tranquada, D. J. Buttrey, and V. Sachan, *Phys. Rev. B* **54**, 12318 (1996).
- [21] M. Cwik, M. Benomar, D. Senff, T. Lorenz, Y. Sidis, and M. Braden, *Phys. Rev. Lett.* **102**, 057201 (2009).
- [22] H. Ulbrich, D. Senff, P. Steffens, O.J. Schumann, Y. Sidis, P. Reutler, A. Revcolevschi, and M. Braden, *Phys. Rev. Lett.* **106**, 157201 (2011).
- [23] A. P. Ramirez, P. Schiffer, S.-W. Cheong, C. H. Chen, W. Bao, T. T. M. Palstra, P. L. Gammel, D. J. Bishop, and B. Zegarski, *Phys. Rev. Lett.* **76**, 3188 (1996).
- [24] C. H. Chen and S.-W. Cheong, *J. Appl. Phys.* **81**, 4326 (1997).
- [25] S. Mori, C. H. Chen, and S.-W. Cheong, *Nature* **392**, 473 (1998).
- [26] M. Coey, *Nature (London)* **430**, 155 (2004).
- [27] J. M. Tranquada, arXiv:cond-mat/0512115v1.
- [28] S. Wakimoto, G. Shirane, Y. Endoh, K. Hirota, S. Ueki, K. Yamada, R. J. Birgeneau, M. A. Kastner, Y. S. Lee, P. M. Gehring and S. H. Lee, *Phys. Rev. B* **60**, R769 (1999).
- [29] S. Wakimoto, R. J. Birgeneau, M. A. Kastner, Y. S. Lee, R. Erwin, P. M. Gehring, S. H. Lee, M. Fujita, K. Yamada, Y. Endoh, K. Hirota and G. Shirane, *Phys. Rev. B* **61**, 3699 (2000).
- [30] M. Matsuda, Y. S. Lee, M. Greven, M. A. Kastner, R. J. Birgeneau, K. Yamada, Y. Endoh, P. Böni, S.-H. Lee, S. Wakimoto and G. Shirane, *Phys. Rev. B* **61**, 4326 (2000).
- [31] S. Wakimoto, S. Ueki, Y. Endoh and K. Yamada, *Phys. Rev. B* **62**, 3547 (2000).
- [32] M. Matsuda, M. Fujita, K. Yamada, R. J. Birgeneau, M. A. Kastner, H. Hiraka, Y. Endoh, S. Wakimoto and G. Shirane, *Phys. Rev. B* **62**, 9148 (2000).
- [33] M. Matsuda, M. Fujita, K. Yamada, R. J. Birgeneau, Y. Endoh and G. Shirane, *Phys. Rev. B* **66**, 174508 (2002).
- [34] G. E. Bacon, *Neutron diffraction*, Clarendon Press, Oxford (1975).
- [35] P. Abbamonte, A. Ruydi, S. Smadici, G. D. Gu, G. A. Sawatzky, and D. L. Feng, *Nat. Phys.* **1**, 155 (2005).
- [36] M. Braden, W. Reichardt, S. Shiryayev and S. Barilo, *Physica C* **378**, 89 (2002).
- [37] M. Braden, L. Pintschovius, T. Uefuji und K. Yamada, *Phys. Rev. B* **72**, 184517 (2005).
- [38] E. Fawcett, *Rev. Mod. Phys.* **60**, 209 (1988).
- [39] E. Fawcett, *Rev. Mod. Phys.* **66**, 25 (1994).
- [40] J. P. Hill, G. Helgesen, and Doon Gibbs, *Phys. Rev. B* **51**, 10336 (1995).
- [41] Y. Takeda, R. Kanno, M. Sakano, O. Yamamoto, M. Takano, Y. Bando, H. Akinaga, K. Takita, and J.B. Goodenough, *Mater. Res. Bull.* **25**, 293 (1990).
- [42] R. J. Cava, B. Batlogg, T. T. Palstra, J. J. Krajewski, W. F. Peck, A. P. Ramirez and L. W. Rupp, *Phys. Rev. B* **43**, 1229 (1991).
- [43] Xiang-Xin Bi and Peter C. Eklund, *Phys. Rev. Lett.* **70**, 2625 (1993).
- [44] A. P. Ramirez, P. L. Gammel, S.-W. Cheong, D. J. Bishop, and P. Chandra, *Phys. Rev. Lett.* **76**, 447 (1996).
- [45] S. Yamanouchi, Y. Taguchi, and Y. Tokura *Phys. Rev. Lett.* **83**, 5555 (1999).
- [46] Tuson Park, Z. Nussinov, K. R. A. Hazzard, V. A. Sidorov, A. V. Balatsky, J. L. Sarrao, S.-W. Cheong, M. F. Hundley, Jang-Sik Lee, Q. X. Jia, and J. D. Thompson, *Phys. Rev. Lett.* **94**, 017002 (2005).
- [47] M. Uchida, K. Ishizaka, P. Hansmann, Y. Kaneko, Y. Ishida, X. Yang, R. Kumai, A. Toschi, Y. Onose, R. Arita, K. Held, O. K. Andersen, S. Shin, and Y. Tokura, *Phys. Rev. Lett.* **106**, 027001 (2011).
- [48] D. J. Buttrey, P. Ganguly, J.M. Honig, C.N.R. Rao, R.R. Schartman, and G.N. Subbanna, *Journal of Sol. State Chem.* **74**, 233 (1988).
- [49] P. I. D. Prabhakaran and A. T. Boothroyd, *J. Crystal Growth* **237**, 815 (2002).
- [50] J. Fontcuberta, G. Longworth, and J. B. Goodenough, *Phys. Rev. B* **30**, 6320 (1984).
- [51] O. Friedt, Diploma thesis, University of Cologne (1998).
- [52] G. H. Lander, P. J. Brown, J. Spalek, and J. M. Honig, *Phys. Rev. B* **40**, 4463 (1989).
- [53] M. Hücker, K. Chung, M. Chand, T. Vogt, J. M. Tranquada, and D. J. Buttrey, *Phys. Rev. B* **70**, 064105 (2004).
- [54] M. Braden, P. Schweiss, G. Heger, W. Reichardt, Z. Fisk, K. Gamayunov, I. Tanaka, and H. Kojima, *Physica C* **223**, 396 (1994).
- [55] P. G. Radaelli, D. G. Hinks, A. W. Mitchell, B. A. Hunter, J. L. Wagner, D. Dabrowski, K. G. Vandervoort, H. K. Viswanathan, and J. D. Jorgensen, *Phys. Rev. B* **49**, 4163 (1994).
- [56] S. M. Hayden, G. H. Lander, J. Zarestky, P. J. Brown, C. Stassis, P. Metcalf, and J. M. Honig, *Phys. Rev. Lett.* **68**, 1061 (1992).
- [57] C. H. Chen, S.-W. Cheong, and A. S. Cooper, *Phys. Rev. Lett.* **71**, 2461 (1993).
- [58] E. D. Isaacs, G. Aeppli, P. Zschack, S.-W. Cheong, H. Williams, and D. J. Buttrey, *Phys. Rev. Lett.* **72**, 3421 (1994).
- [59] K. Yamada, T. Omata, K. Nakajima, Y. Endoh, and S. Hosoya, *Physica (Amsterdam)* **221C**, 355 (1994).
- [60] J. M. Tranquada, D. J. Buttrey, V. Sachan, and J. E. Lorenzo, *Phys. Rev. Lett.* **73**, 1003 (1994).
- [61] J. M. Tranquada, Y. Kong, J. E. Lorenzo, D. J. Buttrey, D. E. Rice, and V. Sachan, *Phys. Rev. B* **50**, 6340 (1994).
- [62] J. E. Lorenzo, J. M. Tranquada, D. J. Buttrey, and V. Sachan, *Phys. Rev. B* **51**, 3176 (1995).
- [63] J. M. Tranquada, J. E. Lorenzo, D. J. Buttrey, and V. Sachan, *Phys. Rev. B* **52**, 3581 (1995).
- [64] P. Wochner, J. M. Tranquada, D. J. Buttrey, and V. Sachan, *Phys. Rev. B* **57**, 1066 (1998).

- [65] J. M. Tranquada, P. Wochner, A. R. Moodenbaugh, and D. J. Buttrey, *Phys. Rev. B* **55**, R6113 (1997).
- [66] V. Sachan, D. J. Buttrey, J. M. Tranquada, J. E. Lorenzo, and G. Shirane, *Phys. Rev. B* **51**, 12742 (1995).
- [67] S.-H. Lee and S.-W. Cheong, *Phys. Rev. Lett.* **79**, 2514 (1997).
- [68] A. Vigliante, M. von Zimmermann, J. R. Schneider, T. Frello, N. H. Andersen, J. Madsen, D. J. Buttrey, Doon Gibbs, and J. M. Tranquada, *Phys. Rev. B* **56**, 8248 (1997).
- [69] H. Yoshizawa, T. Kakeshita, R. Kajimoto, T. Tanabe, T. Katsufuji, and Y. Tokura, *Phys. Rev. B* **61**, R854 (2000).
- [70] S.-H. Lee, J. M. Tranquada, K. Yamada, D. J. Buttrey, Q. Li, and S.-W. Cheong, *Phys. Rev. Lett.* **88**, 126401 (2002).
- [71] Y. Oohara, R. Kajimoto, T. Kakeshita, H. Yoshizawa, T. Tanabe, T. Katsufuji, K. Ishizaka, Y. Taguchi, Y. Tokura, *Physica B* **329** **333**, 725 (2003).
- [72] K. Ishizaka, T. Arima, Y. Murakami, R. Kajimoto, H. Yoshizawa, N. Nagaosa, and Y. Tokura, *Phys. Rev. Lett.* **92**, 196404 (2004).
- [73] R. Kajimoto, T. Kakeshita, H. Yoshizawa, T. Tanabe, T. Katsufuji, Y. Tokura, *Phys. Rev. B* **64**, 144432 (2001).
- [74] C.-H. Du, M. E. Ghazi, Y. Su, I. Pape, P. D. Hatton, S. D. Brown, W. G. Stirling, M. J. Cooper, and S.-W. Cheong, *Phys. Rev. Lett.* **84**, 3911 (2000).
- [75] M. E. Ghazi, P. D. Spencer, S. B. Wilkins, P. D. Hatton, D. Mannix, D. Prabhakaran, A. T. Boothroyd, and S.-W. Cheong, *Phys. Rev. B* **70**, 144507 (2004).
- [76] P.D. Hatton, M.E. Ghazi, S.B. Wilkins, P.D. Spencer, D. Mannix, T. d'Almeida, P. Prabhakaran, A. Boothroyd, S.-W. Cheong, *Physica B* **318**, 289 (2004).
- [77] P.D. Spencer, M.E. Ghazi, S.B. Wilkins, P.D. Hatton, S.D. Brown, D. Prabhakaran, and A.T. Boothroyd, *Eur. Phys. J. B* **46**, 27 (2005).
- [78] C. Schüssler-Langeheine, J. Schlappa, A. Tanaka, Z. Hu, C. F. Chang, E. Schierle, M. Benomar, H. Ott, E. Weschke, G. Kaindl, O. Friedt, G. A. Sawatzky, H.-J. Lin, C. T. Chen, M. Braden and L. H. Tjeng, *Physical Review Letters* **95**, 156402 (2005).
- [79] J. Schlappa, C. F. Chang, E. Schierle, A. Tanaka, R. Feyerherm, Z. Hu, H. Ott, O. Friedt, E. Dudzik, H.-H. Hung, M. Benomar, M. Braden, L. H. Tjeng, and C. Schuessler-Langeheine, arXiv0903.0994.
- [80] Y. Yoshinari, P. C. Hammel, and S.-W. Cheong, *Phys. Rev. Lett.* **82**, 3536 (1999).
- [81] A.C. Komarek, Dissertation, Universität zu Köln (2009).
- [82] A.C. Komarek, P.G. Freemann, and M. Braden, unpublished.
- [83] A. T. Savici, I. A. Zaliznyak, G. D. Gu, and R. Erwin, *Phys. Rev. B* **75**, 184443 (2007).
- [84] L. Pintschovius and W. Reichardt, M. Braden, G. Dhalenne and, A. Revcolevschi, *Phys. Rev. B* **64**, 094510 (2001).
- [85] J. M. Tranquada, K. Nakajima, M. Braden, L. Pintschovius, and R. J. McQueeney, *Phys. Rev. Lett.* **88**, 075505 (2002).
- [86] T. Katsufuji, T. Tanabe, T. Ishikawa, S. Yamanouchi, Y. Tokura, T. Kakeshita, R. Kajimoto, and H. Yoshizawa, *Phys. Rev. B* **60**, R5097 (1999).
- [87] S. H. Han, M. B. Maple, Z. Fisk, S.-W. Cheong, A. S. Cooper, O. Chmaissem, J. D. Sullivan, and M. Marezio, *Phys. Rev. B* **52**, 1347 (1995).
- [88] Guoqing Wu, J. J. Neumeier, C. D. Ling, and D. N. Argyriou, *Phys. Rev. B* **65**, 174113 (2002).
- [89] S. Yamamoto, T. Fujiwara, and Y. Hatsugai *Phys. Rev. B* **76**, 165114 (2007).
- [90] U. Schwingenschlögl, C. Schuster, and R. Frésard, *Europhys. Lett.* **81**, 27002 (2008).
- [91] U. Schwingenschlögl, C. Schuster, and R. Frsard, *Ann. Phys. (Berlin)* **18**, 107 (2009).
- [92] I. M. Abu-Shiekah, O. Bakharev, H. B. Brom, and J. Zaanen *Phys. Rev. Lett.* **87**, 237201 (2001).
- [93] I. M. Abu-Shiekah, O. O. Bernal, A. A. Menovsky, H. B. Brom, and J. Zaanen, *Phys. Rev. Lett.* **83**, 3309 (1999).
- [94] P. G. Freeman, A. T. Boothroyd, D. Prabhakaran, M. Enderle, and C. Niedermayer, *Phys. Rev. B* **70**, 024413 (2004).
- [95] K. Nakajima, K. Yamada, S. Hosoya, T. Omata, and Y. Endoh, *J. Phys. Soc. Jpn.* **62**, 4438 (1993).
- [96] J. M. Tranquada, P. Wochner, and D. J. Buttrey, *Phys. Rev. Lett.* **79**, 2133 (1997).
- [97] P. Bourges, Y. Sidis, M. Braden, K. Nakajima, and J. M. Tranquada, *Phys. Rev. Lett.* **90**, 147202 (2003).
- [98] A. T. Boothroyd, D. Prabhakaran, P. G. Freeman, S. J. S. Lister, M. Enderle, A. Hiess, and J. Kulda, *Phys. Rev. B* **67**, 100407 (2003).
- [99] A. T. Boothroyd, P. G. Freeman, D. Prabhakaran, A. Hiess, M. Enderle, J. Kulda, and F. Altorfer, *Phys. Rev. Lett.* **91**, 257201 (2003).
- [100] Hyungje Woo, A. T. Boothroyd, K. Nakajima, T. G. Perring, C. D. Frost, P. G. Freeman, D. Prabhakaran, K. Yamada, and J. M. Tranquada, *Phys. Rev. B* **72**, 064437 (2005).
- [101] C. D. Batista, G. Ortiz, and A. V. Balatsky, *Phys. Rev. B* **64**, 172508 (2001).
- [102] R. Kajimoto, K. Ishizaka, H. Yoshizawa, and Y. Tokura, *Phys. Rev. B* **67**, 014511 (2003).
- [103] P. G. Freeman, A. T. Boothroyd, D. Prabhakaran, C. D. Frost, M. Enderle, and A. Hiess, *Phys. Rev. B* **71**, 174412 (2005).
- [104] P. G. Freeman, D. Prabhakaran, K. Nakajima, A. Stunault, M. Enderle, C. Niedermayer, C. D. Frost, K. Yamada, and A. T. Boothroyd, *Phys. Rev. B* **83**, 094414 (2011).
- [105] M. Hücker, M. v. Zimmermann, R. Klingeler, S. Kiele, J. Geck, S. N. Bakehe, J. Z. Zhang, J. P. Hill, A. Revcolevschi, D. J. Buttrey, B. Bchner, and J. M. Tranquada, *Phys. Rev. B* **74**, 085112 (2006).
- [106] M. Hücker, M. v. Zimmermann, and G. D. Gu, *Phys. Rev. B* **75**, 041103 (2007).
- [107] X. Yu, T. Arima, S. Seki, T. Asaka, K. Kimoto, Y. Tokura, and Y. Matsui, *J. of Phys. Soc. Jpn* **77**, 093709 (2008).
- [108] B. Renker, F. Gompf, E. Gering, N. Nuecker, D. Ewert, W. Reichardt, and H. Rietschel, *Z. Phys.* **67** 15 (1987).
- [109] B. Renker, F. Gompf, E. Gering, D. Ewert, H. Rietschel, and A. Di-janoux, *Z. Phys.* **73** 309 (1988).
- [110] B. Renker, F. Gompf, E. Gering, G. Roth, D. Ewert, H. Rietschel, and H. Mutka, *Z. Phys.* **71** 437 (1988).
- [111] L. Pintschovius and W. Reichardt, in *Neutron Scattering in Layered Copper-Oxide Superconductors*, ed. by A. Furrer, *Phys. and Chem. of Materials with Low-Dim. Structures*, Vol. 20 (Kluwer Academic Publ., Dordrecht, 1998), 165.
- [112] L. Pintschovius and M. Braden, *Phys. Rev. B* **60**, R15039 (1999).
- [113] R. J. McQueeney, Y. Petrov, T. Egami, M. Yethiraj, G. Shirane, and Y. Endoh, *Phys. Rev. Lett.* **82**, 628 (1999).
- [114] R. J. McQueeney, J. L. Sarrao, P. G. Pagliuso, P. W. Stephens, and R. Osborn, *Phys. Rev. Lett.* **87**, 077001 (2001).
- [115] W. Reichardt, *J. Low Temp. Phys.* **105**, 807(1996).
- [116] J.-H. Chung, T. Egami, R. J. McQueeney, M. Yethiraj, M. Arai, T. Yokoo, Y. Petrov, H. A. Mook3, Y. Endoh, S. Tajima, C. Frost, and F. Dogan, *Phys. Rev. B* **67**, 014517 (2003).
- [117] H. Uchiyama, A. Q. R. Baron, S. Tsutsui, Y. Tanaka, W.-Z. Hu, A. Yamamoto, S. Tajima, and Y. Endoh, *Phys. Rev. Lett.* **92**, 197005 (2004).
- [118] M. d'Astuto, P. K. Mang, P. Giura, A. Shukla, P. Ghigna, A. Mirone, M. Braden, M. Greven, M. Krisch, and F. Sette *Phys. Rev. Lett.* **88**, 167002 (2002).
- [119] D. Reznik, L. Pintschovius, M. Ito, S. Iikubo, M. Sato, H. Goka, M. Fujita, K. Yamada, G. D. Gu and J. M. Tranquada, *Nature* **440**, 1170 (2006).
- [120] S. L. Chaplot, W. Reichardt, L. Pintschovius, and N. Pyka *Phys. Rev. B* **52**, 7230-7242 (1995).
- [121] Y. Moritomo, K. Higashi, K. Matsuda, and A. Nakamura, *Phys. Rev. B* **55**, R14725 (1997).
- [122] P. Ganguly and S. Ramasesha, *Magnetism Letters* **1**, 131 (1980).
- [123] Y. Shimada, S. Miyasaka, R. Kumai, and Y. Tokura, *Phys. Rev. B* **73**, 134424 (2006).
- [124] Y. Furukawa, S. Wada, and Y. Yamada, *J. of Phys. Soc. of Jpn.* **62**, 1127 (1993).
- [125] K. Yamada, M. Matsuda, Y. Endoh, B. Keimer, R. J. Birgenau, S. Onodera, J. Mizukawa, T. Matsuura, and G. Shirane, *Phys. Rev. B* **39**, 2336 (1989).
- [126] P. M. Raccah and J. B. Goodenough, *Phys. Rev.* **155**, 932 (1967).
- [127] N. Hollmann, M. W. Haverkort, M. Cwik, M. Benomar, M. Reuther, A. Tanaka, and T. Lorenz, *New J. Phys.* **10**, 023018 (2008).
- [128] R. Le Toquin, Dissertation, Université de Rennes (2003).
- [129] A. Nemudry, P. Rudolf, and R. Schöllhorn, *Sol. State Ionics* **109**, 213 (1998).
- [130] R. A. M. Ram, P. Ganguly, and C. N. R. Rao, *Mat. Res. Bull.* **23**, 501 (1988).
- [131] T. Matsuura, J. Mizusaki, S. Yamauchi, and K. Fueki, *J. Appl. Phys.* **23**, 1143 (1984).
- [132] M. Haider, diploma thesis, Universität zu Köln, (2005).
- [133] T. Kajitani, S. Hosoya, K. Hiraga, and T. Fukuda, *J. Phys. Soc. Japan*

- 59, 562 (1989).
- [134] T. Thio, T. R. Thurston, N. W. Preyer, P. J. Picone, M. A. Kastner, H. P. Janssen, D. R. Gabbe, C. Y. Chen, R. J. Birgeneau, and A. Aharony, *Phys. Rev. B* **38**, 905 (1988).
- [135] M. Braden, G. André, S. Nakatsuji und Y. Maeno, *Phys. Rev. B* **58**, 847 (1998).
- [136] I. A. Zaliznyak, J. P. Hill, J. M. Tranquada, R. Erwin, and Y. Moritomo, *Phys. Rev. Lett.* **85**, 4353 (2000).
- [137] I. A. Zaliznyak, J. M. Tranquada, R. Erwin, and Y. Moritomo, *Phys. Rev. B* **64**, 195117 (2001).
- [138] M. Cwik, Dissertation, Universität zu Köln (2007).
- [139] H. Wu and T. Burnus, *Phys. Rev. B* **80**, 081105 (2009).
- [140] N. Hollmann, M. Haverkort, M. Benomar, M. Cwik, M. Braden, and T. Lorenz, *Phys. Rev. B* **84**, 174435 (2011).
- [141] M. Itoh, M. Mori, Y. Moritomo, and A. Nakamura, *Physica B* **259-261**, 997 (1999).
- [142] J. Wang, W. Zhang, and D. Y. Xing, *Phys. Rev. B* **62**, 14140 (2000).
- [143] T. Matsuura, J. Tabuchi, J. Mizusaki, S. Yamauchi, and K. Fueki, *J. Phys. Chem. Solids* **49**, 1409 (1988).
- [144] K. Horigane, H. Hiraka, T. Uchida, K. Yamada, and J. Akimitsu, *J. Phys. Soc. Jpn.* **76**, 114715 (2007).
- [145] K. Horigane, H. Nakao, Y. Kousaka, T. Murata, Y. Noda, Y. Murakami, and J. Akimitsu, *J. Phys. Soc. Jpn.* **77**, 044601 (2008).
- [146] C. F. Chang, Z. Hu, Hua Wu, T. Burnus, N. Hollmann, M. Benomar, T. Lorenz, A. Tanaka, H.-J. Lin, H. H. Hsieh, C. T. Chen, and L. H. Tjeng, *Phys. Rev. Lett.* **102**, 116401 (2009).
- [147] L. M. Helme, A. T. Boothroyd, D. Prabhakaran, F.R. Wondre, C. D. Frost, and J. Kulda, *Physica B* **350**, e273 (2004).
- [148] L. M. Helme, A. T. Boothroyd, R. Coldea, D. Prabhakaran, C. D. Frost, D. A. Keen, L. P. Regnault, P. G. Freeman, M. Enderle, and J. Kulda, *Phys. Rev. B* **80**, 134414 (2009).
- [149] A. Maignan, V. Caignaert, B. Raveau, D. Khomskii, and G. Sawatzky, *Phys. Rev. Lett.* **93**, 026401 (2004).
- [150] S.-W. Cheong, A. S. Cooper, Jr. L. W. Rupp, B. Battlog, J. D. Thomson, and Z. Fisk, *Phys. Rev. B* **44**, 9739 (1991).
- [151] M. Braden, M. Meven, W. Reichardt, L. Pintschovius, M. T. Fernandez-Diaz, G. Heger, F. Nakamura, and T. Fujita, *Phys. Rev. B* **63**, 140510 (2001).
- [152] A. T. Boothroyd, P. Babkevich, D. Prabhakaran, and P. G. Freeman, *Nature* **471**, 341 (2011).
- [153] N. Sakiyama, I. A. Zaliznyak, S.-H. Lee, Y. Mitsui, and H. Yoshizawa, *Phys. Rev. B* **78**, 180406 (2008).
- [154] P. Babkevich, D. Prabhakaran, C. D. Frost, and A. T. Boothroyd, *Phys. Rev. B* **82**, 184425 (2010).
- [155] Y. Tokura and N. Nagaosa, *Science* **288**, 462 (2000).
- [156] Y. Tokura and Y. Tomioka, *Journal of Magnetism and Magnetic Materials* **200**, 1 (1999).
- [157] A. J. Millis, P. B. Littlewood, and B. I. Shraiman, *Phys. Rev. Lett.* **74**, 5144 (1995).
- [158] S. Murakami and N. Nagaosa, *Phys. Rev. Lett.* **90**, 197201 (2003).
- [159] M. Uehara, S. Mori, C. H. Chen, and S.-W. Cheong, *Nature* **399**, 560 (1999).
- [160] A. Moreo, S. Yunoki, and E. Dagotto, *Science* **283**, 2034 (1999).
- [161] F. M. Woodward, J. W. Lynn, M. B. Stone, R. Mahendiran, P. Schiffer, J. F. Mitchell, D. N. Argyriou, and L. C. Chapon, *Phys. Rev. B* **70**, 174433 (2004).
- [162] G. C. Milward, M. J. Calderón, and P. B. Littlewood, *Nature* **433**, 607 (2005).
- [163] C. Şen, G. Alvarez, and E. Dagotto, *Phys. Rev. Lett.* **98**, 127202 (2007).
- [164] E. O. Wollan and W. C. Koehler, *Phys. Rev.* **100**, 545 (1955).
- [165] J. B. Goodenough, *Phys. Rev.* **100**, 564 (1955).
- [166] P. G. Radaelli, D. E. Cox, M. Marezio, and S.-W. Cheong, *Phys. Rev. B* **55**, 3015 (1997).
- [167] A. Daoud-Aladine, J. Rodríguez-Carvajal, L. Pinsard-Gaudart, M. T. Fernández-Díaz, and A. Revcolevschi, *Phys. Rev. Lett.* **89**, 097205 (2002).
- [168] Y. Moritomo, Y. Tomioka, A. Asamitsu, Y. Tokura, and Y. Matsui, *Phys. Rev. B* **51**, 3297 (1995).
- [169] M. Tokunaga, N. Miura, Y. Moritomo, and Y. Tokura, *Phys. Rev. B* **59**, 11151 (1999).
- [170] P. Reutler, O. Friedt, B. Büchner, M. Braden, and A. Revcolevschi, *J. Cryst. Growth* **249**, 222 (2003).
- [171] B. J. Sternlieb, J. P. Hill, U. C. Wildgruber, G. M. Luke, B. Nachumi, Y. Moritomo, and Y. Tokura, *Phys. Rev. Lett.* **76**, 2169 (1996).
- [172] S. Larochelelle, A. Mehta, N. Kaneko, P. K. Mang, A. F. Panchulla, L. Zhou, J. Arthur, and M. Greven, *Phys. Rev. Lett.* **87**, 095502 (2001).
- [173] P. Mahadevan, K. Terakura, and D. D. Sarma, *Phys. Rev. Lett.* **87**, 066404 (2001).
- [174] S. B. Wilkins, P. D. Spencer, P. D. Hatton, S. P. Collins, M. D. Roper, D. Prabhakaran, and A. T. Boothroyd, *Phys. Rev. Lett.* **91**, 167205 (2003).
- [175] S. S. Dhesi, A. Mirone, C. De Nadai, P. Ohresser, N. B. Brookes, P. Reutler, A. Revcolevschi, A. Tagliaferri, O. Toulemonde, and G. van der Laan, *Phys. Rev. Lett.* **92**, 056402 (2004).
- [176] S. Larochelelle, A. Mehta, L. Lu, P. K. Mang, O. P. Vajk, N. Kaneko, J. W. Lynn, L. Zhou, and M. Greven, *Phys. Rev. B* **71**, 024435 (2005).
- [177] Hua Wu, C. F. Chang, O. Schumann, Z. Hu, J. C. Cezar, T. Burnus, N. Hollmann, N. B. Brookes, A. Tanaka, M. Braden, L. H. Tjeng, and D. I. Khomskii, *Phys. Rev. B* **84**, 155126 (2011).
- [178] D. Senff, F. Krüger, S. Scheidl, M. Benomar, Y. Sidis, F. Demmel, and M. Braden, *Phys. Rev. Lett.* **96**, 257201 (2006).
- [179] D. Senff, O. Schumann, M. Benomar, M. Kriener, T. Lorenz, Y. Sidis, K. Habicht, P. Link, and M. Braden, *Phys. Rev. B* **77**, 184413 (2008).
- [180] Z. Jirak, S. Krupicka, Z. Simsa, M. Dlouha, and S. Vraatislav, *J. of Magn. and Magn. Mat.* **53**, 153 (1985).
- [181] J. Damay, Z. Jirak, M. Hervieu, C. Martin, A. Maignan, B. Raveau, G. André, and F. Bourrée, *J. of Magn. and Magn. Mat.* **190**, 221 (1998).
- [182] Z. Jirak, F. Damay, M. Hervieu, C. Martin, B. Raveau, G. André, and F. Bourrée, *Phys. Rev. B* **61**, 1181 (2000).
- [183] D. Senff, P. Reutler, M. Braden, O. Friedt, D. Bruns, A. Cousson, F. Bourée, M. Merz, B. Büchner, and A. Revcolevschi, *Phys. Rev. B* **71**, 024425 (2005).
- [184] H. Ulbrich, F. Krüger, A. A. Nugroho, D. Lamago, Y. Sidis, and M. Braden, *Phys. Rev. B* **84**, 094453 (2011).
- [185] C.H. Chen, S. Mori, and S.-W. Cheong, *J. Phys. IV France* **9**, PR10-307 (1999).
- [186] Y. S. Lee, T. Arima, S. Onoda, Y. Okimoto, Y. Tokunaga, R. Mathieu, X. Z. Yu, J. P. He, Y. Kaneko, Y. Matsui, N. Nagaosa, and Y. Tokura, *Phys. Rev. B* **75**, 144407 (2007).
- [187] R. Wang and J. Gui, *Phys. Rev. B* **61**, 18 (2000).
- [188] T. Kimura, K. Hatsuda, Y. Ueno, R. Kajimoto, H. Mochizuki, H. Yoshizawa, T. Nagai, Y. Matsui, A. Yamazaki, and Y. Tokura, *Phys. Rev. B* **65**, 020407 (2001).
- [189] J. C. Loudon, S. Cox, A. J. Williams, J. P. Attfield, P. B. Littlewood, P. A. Midgley, and N. D. Mathur, *Phys. Rev. Lett.* **94**, 097202 (2005).
- [190] L. Brey and P.B. Littlewood, *Phys. Rev. Lett.* **95**, 117205 (2005).
- [191] L. Brey, *Phys. Rev. Lett.* **92**, 127202 (2004).
- [192] Z. P. Luo, D. J. Miller, and J. F. Mitchell, *Phys. Rev. B* **71**, 014418 (2005).
- [193] T. A. W. Beale, P. D. Spencer, P. D. Hatton, S. B. Wilkins, M. v. Zimmermann, S. D. Brown, D. Prabhakaran, and A. T. Boothroyd, *Phys. Rev. B* **72**, 064432 (2005).
- [194] X. Z. Yu, R. Mathieu, T. Arima, Y. Kaneko, J. P. He, M. Uchida, T. Asaka, T. Nagai, K. Kimoto, A. Asamitsu, Y. Matsui, and Y. Tokura, *Phys. Rev. B* **75**, 174441 (2007).
- [195] T. Nagai, T. Kimura, A. Yamazaki, Y. Tomioka, K. Kimoto, Y. Tokura, Y. Matsui, *Phys. Rev. B* **68**, 1092405 (2003).
- [196] A. Nucara, P. Maselli, P. Calvani, R. Sopracase, M. Ortolani, G. Gruener, M. Castellì Guidi, U. Schade, and J. García, *Phys. Rev. Lett.* **101**, 066407 (2008).
- [197] D. Koumoulis, N. Panopoulos, A. Reyes, M. Fardis, M. Pissas, A. Douvalis, T. Bakas, D. N. Argyriou, and G. Papavassiliou, *Phys. Rev. Lett.* **104**, 077204 (2010).
- [198] P. G. Radaelli, D. E. Cox, L. Capogna, S.-W. Cheong, and M. Marezio, *Phys. Rev. B* **59**, 14440 (1999).
- [199] M. T. Fernández-Díaz, J. L. Martínez, J. M. Alonso, and E. Herrero, *Phys. Rev. B* **59**, 1277 (1999).
- [200] M. Hervieu, A. Maignan, C. Martin, N. Nguyen, and B. Raveau, *Chem. Mater.* **13**, 1356 (2001).
- [201] M. Pissas and G. Kallias, *Phys. Rev. B* **68**, 134414 (2003).
- [202] M. Pissas, I. Margiolaki, K. Prassides, and E. Suard, *Phys. Rev. B* **72**, 064426 (2005).
- [203] Grenier, S. and Kiryukhin, V. and Cheong, S.-W. and Kim, B. G. and Hill, J. P. and Thomas, K. J. and Tonnerre, J. M. and Joly, Y. and Staub, U.

- and Scagnoli, V. Phys. Rev. B **75**, 085101 (2007).
- [204] I. V. Solov'yev and K. Terakura, Phys. Rev. Lett. **83**, 2825 (1999).
- [205] J. van den Brink, G. Khaliullin, and D. Khomskii, Phys. Rev. Lett. **83**, 5118 (1999).
- [206] I. V. Solov'yev, Phys. Rev. Lett. **91**, 177201 (2003).
- [207] I. V. Solov'yev, Phys. Rev. B **63**, 174406 (2001).
- [208] L. Brey, Phys. Rev. B **71**, 174426 (2005).
- [209] M. Daghofer, A. M. Oles, D. R. Neuber, and W. von der Linden, Phys. Rev. B **73**, 104451 (2006).
- [210] H. Ulbrich, P. Steffens, D. Lamago, Y. Sidis, and M. Braden, arXiv1112.1799.
- [211] W. Norimatsu and Y. Koyama, Phys. Rev. B **74**, 085113 (2006).
- [212] W. Norimatsu and Y. Koyama, Phys. Rev. B **75**, 235121 (2007).
- [213] F. Ye, Songxue Chi, J. A. Fernandez-Baca, A. Moreo, E. Dagotto, J. W. Lynn, R. Mathieu, Y. Kaneko, Y. Tokura, and Pengcheng Dai, Phys. Rev. Lett. **103**, 167202 (2009).
- [214] Y. Endoh, H. Hiraka, Y. Tomioka, Y. Tokura, N. Nagaosa, and T. Fujiwara, Phys. Rev. Lett. **94**, 017206 (2005).
- [215] F. Ye, Pengcheng Dai, J. A. Fernandez-Baca, D. T. Adroja, T. G. Perring, Y. Tomioka, and Y. Tokura, Phys. Rev. B **75**, 144408 (2007).
- [216] see discussion in: S. Petit, M. Hennion, F. Moussa, D. Lamago, A. Ivanov, Y. M. Mukovskii, and D. Shulyatev, Phys. Rev. Lett. **102**, 207201 (2009).
- [217] M. Braden, O. Friedt, Y. Sidis, P. Bourges, M. Minakata, and Y. Maeno, Phys. Rev. Lett. **88**, 197002 (2002).
- [218] Y. Sidis, M. Braden, P. Bourges, B. Hennion, S. NishiZaki, Y. Maeno, and Y. Mori, Phys. Rev. Lett. **83**, 3320 (1999).